NsG-6

MODIFIED TECHNIQUE FOR MEASURING DIELECTRIC CONSTANTS USING A RECTANGULAR CAVITY RESONATOR

by

J. K. Sinha
Electrical Engineering Department
Rice University
Houston, Texas

33393

SUMMARY

A modified technique using a partially filled rectangular cavity-resonator is described. This technique is analogous to the technique described earlier by the author in which a partially filled tunable cylindrical cavity resonator is employed. The theory and the method of operation of this technique are discussed and the special advantages resulting from its use are pointed out.

Introduction

A number of resonance methods of dielectric measurements have been described earlier by Lamb[1], Horner[2], Collie et al[3] and Sinha[4]. In Lamb's method one needs a disc sample with an accurate fit with the diameter of the Ho_{1n} cylindrical cavity resonator used. Hotston[5], however, has worked out a perturbation relation by which one may evaluate the real part of the permittivity in the Lamb's technique for disc samples having a considerable clearance between themselves and the inner walls of the cavity. He does not, however, investigate the possibility of the evaluation of loss-tangents for such samples and hence one needs to use a sample with a good fit for reliable evaluation of loss-tangent. Horner uses rod samples longitudinally filling a non-tunable E_{010} cavity while Collie uses a thin capillary filled with water extending coaxially along the entire length of a Ho_{1n} cavity for the evaluation of the dielectric properties of water. Sinha[4] and Brown, however, have described a technique using a Ho_{1n} cylindrical cavity where the samples are in the form of rods which partially fill the cavity along its axis. This technique offers the facility that the sample need not have an accurate fit with respect to any one dimension of the cavity and also the cavity being tunable, all the measurements could be made at any fixed frequency.

In practice this method proved very successful except that the advantages obtained resulted from an increased computational work due to the complex solution of the Maxwell's fields inside the system and also that one is limited only to rod samples.

As it is quite often the case that the dielectric materials are available in the form of plane sheets, it was felt desirable therefore, to have a technique which could have most of the advantages of the aforementioned technique[4] and could employ a sample in the form of a sheet or plane slab for the derivation of its electrical properties. Hence, a partially filled technique has been developed using a rectangular cavity resonator formed by using a standard x-band waveguide, in which the samples would be in the form of thin sheets partially filled the cavity along its length and having their widths equal to the narrow dimension of the guide. The sample could either be in contact with the sidewall or alternatively be in the center of the cross-section of the guide. The other end of the guide is closed by a tuning plunger. The cavity is coupled to the generator and the detector through holes in the side walls.

It must be mentioned here, however, that although one of the major advantages available by using the cylindrical cavity resonator method, i.e., of having specimens that do not need to have an accurate fit with any of the cavity dimensions, is not present, it has all the other desirable features. In fact, as the solution of the Maxwell's equations for this system turns out to be simpler than the solution for the cylindrical resonator system, the expressions for the various parameters in terms of the measurable quantities (the guide wavelength in the partially filled portion and the Q factors for two different insertions of the sample differing by half a wavelength) turn out to be much simpler, thereby, reducing the computational labor considerably as compared to the technique described previously[4]. In addition, as the cavity in this case is operated in its dominant mode and

the dimensions of the cavity are such that theproblems due to the presence of unwanted modes are not encountered. This is a definite advantage over the author's previous technique in which the experiment is done in the HO_{1n} mode which is not the dominant mode of the cylindrical cavity. Hence, special precautions are taken in dimensioning the cavity for the suppression of the unwanted modes.

It is also believed that the limitation of having the sample width equal to the narrow dimension of the cavity is not a great inconvenience due to the simple shape of the sample and the convenient size of the cavity's cross section.

In addition, the samples can either be in the center where the electric field and hence the perturbation is the maximum or alternately the sample could be at the side walls when the perturbation is small. One can use the former configuration for the investigations of low permittivity and low electric loss materials while the latter configuration will offer advantages for the materials having high permittivities and higher electrical losses.

Outline of the Method

The procedure involved in the evaluation of the various parameters are exactly the same as in the author's previous method and is outlined below.

The real part of the permittivity is evaluated from the measured value of the wavelength inside the partially filled portion of the cavity and the loss-tangenet is obtained by measuring the Q of the cavity corresponding to the two insertions of the dielectric specimen differing by half a guide wavelength.

The photograph of the cavity system used in the present work is shown in Fig. 1. The cavity is made from a length of standard X-band waveguide and is resonant in its dominant HO_{14} mode. At one of the closed ends there is a provision for the tuning of the cavity by the accurately controlled movement of theplunger while at the other end provision has been made for the controlled insertion of the dielectric sample inside the cavity either along its center or along its sidewall. This end of the cavity is terminated by a thick backing plate having recesses cut both at the center and along the ends. Provision has been made for closing either the central recess or the end recess on this plate depending on whether one is inserting the sample through the center or through the side. The width of these recesses can also be varied by screwing in rectangular plates in order to be able to investigate samples having different thicknesses. The other end of the sample is held by a screw in a recess on another fixed plate which is attached to the shaft of a micrometer in order to insert the sample inside the cavity by measured amounts. The backing plate on the dielectric side is chosen sufficiently thick so that no power may leak out of the cavity through the recesses provided for the insertion of the samples. The coupling to the generator and the detector is made through holes cut in the sidewalls.

The wavelength in the partially filled portion is evaluated from the curve obtained by plotting the total length of the cavity system against the length of insertion of the dielectric and the resulting curve is identical in form to those obtained by the well known Feenberg[6] method.

The quality factor is evaluated at a fixed frequency from the resonance curve by detuning the cavity with the help of the tuning plunger. The

expression correlating the half width frequency Δf with the corresponding $\Delta \ell$ is obtained by differentiating the equation as shown in the appendix.

Theory

The cavity system under discussion is basically as shown in Fig. 2 consisting of a length "d" of the empty waveguide and a length "ℓ" of the partially filled waveguide. The junction between the two waveguides may be assumed to be loss-free and as such can be represented by an ideal transformer with a turn ration "n" at certain characteristic reference planes[7]. The equivalent circuit of the system can, therefore, be shown as in Fig. 3 where d_o and ℓ_o are taken to be the distances of the reference planes from the actual junction in order to account for the phase changes introduced. The condition that the circuit of Fig. 3 should resonate at a given free space wavelength is:

$$\tan\beta_1(d+d_o) = -n^2 z_2/z_1 \tan\beta_2(\ell+\ell_o) \qquad (1)$$

where β_1, β_2 are the phase change co-efficients and Z_1, Z_2 the wave impedances in the empty and partially filled portions of the cavity respectively. Now, instead of specifying both the impedances in the above equation one can specify only one impedance, say Z_1 and put $n = 1$. The value of Z_2/Z_1 is fixed. Hence Z_2/Z_1 can be used as the third parameter to give the value of the reflection coefficient at a discontinuity. Such a procedure has been justified by Collin and Brown[8] by using Schwinger's variational method and also by Sinha[9] by using a different approach.

The equation (1), therefore, is now written as:

$$\tan\beta_1(d+d_o) = -z_2/z_1 \tan\beta_2(\ell+\ell_o) \qquad (2)$$

or $$\tan \beta_1 d' = z_2/z_1 \tan \beta_2 l' \quad \text{---------} \quad (3)$$

where $d' = d + d_o$ and $l' = l + l_o$

The above equation coupled with Feenberg's theory can therefore be used to predict the form of dependence between l' and d'. In the present application it is most convenient to plot $(d' + l')$ against l'. The curve of $(d' + l')$ against l' has the shape shown in Fig. 4. The curve of $(d + l)$ vs l will also have the same slope but will be displaced by an amount l_o along the horizontal axis and by an amount $(d_o + l_o)$ along the vertical axis. The man slope of the curve, i.e., the slope of the dotted line, is given by $\frac{(\beta_2 - \beta_1)}{\beta_2}$. The value of this slope can be measured from experiment and β_1 can be simply calculated. This enables the determination of β_2, i.e., the phase change coefficient in the partially filled portion. Hence, the only remaining step in the determination of ϵ_r is the correlation of β_2 with ϵ_r.

It may also be mentioned that the values of d_o and l_o, defined in Eq. (3), can be determined from the curve of $(d + l)$ vs l as it can be shown that corresponding to its point of maximum slope,

$$d + l + d_o + l_o = p\lambda_1/4 + q\lambda_2/4 \quad \text{------} \quad (4)$$

and

$$l + l_o = q\lambda_2/4 \quad \text{----------} \quad (5)$$

p and q in the above equations are integers and easily deducible from the known values of λ_1, λ_2 and the physical length of the cavity. The values of d_o and l_o are needed in some of the derivations as will be seen later.

The foregoing discussion is valid for both the cases, i.e., when the sample is in contact with the side wall and also when the sample is at the center of the cross section.

Evaluation of ϵ_r from $\beta_2(\lambda_2)$

(i) Case when the sample is in contact with the sidewall

The arrangement for this case is shown in Fig. 5. Pincherley[10] has considered such a system and obtained the characteristic equations for the HO_1 mode supporting E_x, H_y and H_z. The same equation, however, is more readily obtained from transverse resonance conditions and is written as

$$\phi_1(k_1 t) = -\phi_2(k_2 t) \qquad (6)$$

where $\phi_1(k_1 t) = \tan k_1 t / k_1 t$ and $\phi_2(k_2 t) = \tan k_2(a-t)/k_2 t$

K_1 and K_2 appearing in the above equations are of the nature of propagation constants and are given by:

$$K_1^2 = \omega^2 \mu_0 \epsilon_1 - \beta^2 \qquad (7)$$

$$k_2^2 = \omega^2 \mu_0 \epsilon_0 - \beta^2 \qquad (8)$$

where ϵ_1 is the permittivity of the sample and β is the phase change coefficient inside the guide system.

The procedure for the evaluation of ϵ_r from β is as follows. K_2 is first obtained from Eq. (8) and K_1 may then be evaluated from the transcedental Eq. (6). The substitution of K_1 in the Eq. (7) now enables the determination of ϵ_1 or ϵ_1/ϵ_0, the relative permittivity of the sample.

In practice, however, it is desirable to have charts from which the dielectric parameters could be read directly, given the required experimental data. Such charts have been computed for a range of the sample thicknesses and for three different frequencies, i.e., 8 Kmc, 10 Kmc and 12 Kmc, and

are given in Figs. 6, 7 and 8 respectively.

(ii) The sample along the center of the cross section of the guide.

The cross section of the arrangement having the sample along the center of the guide is shown in Fig. (9). Such a system has been considered earlier by Vartanian[12] et al, who obtained the characteristic equation for this system, supporting either E or H mode. However, the same equation is obtained simply by the transverse resonance conditions and is given for the dominant HO_1 mode as

$$\phi_1'(K_1't') = 2d/t' \cdot \phi_2'(K_2'd) \quad \text{---------} \quad (9)$$

where $\phi_1'(K_1't') = \dfrac{\cot K_1't'/2}{K_1't'/2}$ and $\phi_2'(K_2'd) = \tan K_2'd/K_2'd$

Once again, K_1' and K_2' in Eq. (9) are given by the following relations:

$$K_1'^2 = \omega_0'^2 \mu_0 \epsilon_1 - \beta'^2 \quad \text{-----} \quad (10)$$

$$K_2'^2 = \omega_0'^2 \mu_0 \epsilon_0 - \beta'^2 \quad \text{-----} \quad (11)'$$

β' being the phase change coefficient for this configuration.

The procedure for evaluating ϵ_r from Eqs. (9-11) are the same as for the previous case. The theoretical charts, for directly reading ϵ_r from the experimental data, have been prepared for a range of sample sizes for this case and are shown in Figs. (10-12) for the respective frequencies of 8, 10 and 12 Kmc/s.

Limitation on the Thickness of the Sample

It must be mentioned at this stage that although there is no specification regarding the precise value of the thickness to be measured by either of these methods, a limitation to the thickness of the sample is imposed by the condition

of single mode propagation because above a certain value of the thickness, the cavity in addition to the dominant mode can support the next higher mode and the experimental determination of wavelength is complicated as the curve of $d + \ell$ vs ℓ becomes very irregular for such a case. Hence, the thickness of the sample corresponding to any particular ϵ_r should be such that the HO_2 mode is cut off.

This value of ϵ_r for HO_2 cut-off is determined from Eqs. (6-8) for the side filled case by putting β equal to zero in the eqs. 7 and 8, as the form of the characteristic equation remains unchanged for the HO_2 mode.[10]

For the case of the centrally filled system, however, one cannot use Dq. (9) as the characteristic equation for HO_2 mode is given by[11,12]

$$\frac{\tan k_1' t'/2}{k_1'} = -\tan k_2' d'/k_2' \quad - - - \qquad (12)$$

Now, by using Eqs. (10-12) and putting β' equal to zero, one can evaluate the maximum value of ϵ_r corresponding to any thickness for keeping the HO_2 mode at cutoff.

It must be noted, in addition, that K_2 and K_2' in Eqs. (8) and (11) become imaginary if β or β' exceeds β_o or β_o', or in other words, the guide wavelength becomes smaller than the free space wavelength. Hence there is a limiting value of the thickness of the sample for any particular ϵ_r beyond which one needs to evaluate the hyperbolic functions for the evaluation of the dielectric parameters. This limiting value of ϵ_r for any thickness for the two cases may be obtained from Eqs. (6-8) and Eqs. (9-11) by putting $\beta = \beta_o$ and $\beta' = \beta_o'$ into them respectively.

The curves showing the maximum value of ϵ_r vs. thickness for the HO_2

cutoff and for the use of only real functions for the side and centrally loaded cases are shown in Fig. (13) and (14) respectively.

The Use of Hyperbolic Functions

It can be seen from Fig. (13) and (14) that the condition for K_2 to be real gives a lower limiting value of ϵ_r corresponding to any thickness as compared to the value obtained for the HO_2 cutoff. Hence, it is seen that in the regions between the two limiting curves, one can get single mode propagation but an imaginary value of K_2'. Hence it is interesting to solve for the hyperbolic functions in this region as the $(d + \ell)$ vs ℓ curve is undistorted and enables the accurate evaluation of the guide wavelength.

Consider first the side-filled configuration. K_2 in Eq. (8) now becomes imaginary, say equal to jK_2. Hence, in the Eq. (6) $\Phi_2 (K_2 t)$ becomes equal to $\frac{\tan h\, K_2 t}{K_2 t}$ while $\Phi_1(K_1 t)$ remains unchanged, as K_1 remains real due to the large values of ϵ_r involved. The procedure for evaluating ϵ_r, however, remains unaltered except for the evaluation of $\tanh K_2 t$ in place of $\tan K_2 t$. Similarly, for the centrally loaded configuration K_2' in Eq. (11) turns imaginary and $\Phi_2' (K_2' d)$ becomes equal to $\frac{\tanh K_2' d}{K_2' d}$ while $\Phi_1' (K_1' t)$ remains unaltered.

There is no theoretical limitation for not using these hyperbolic relations for the regions of the higher H mode propagations. The limitation is imposed, however, from the difficulty in obtaining an undistorted experimental $(d + \ell)$ vs ℓ curve corresponding to HO_1 mode propagation in these circumstances.

The examination of Figs. (13) and (14) shows that the use of hyperbolic functions is profitable only for the centrally loaded configuration as in the side loaded configuration the conditions of single mode propagation and

restriction to only real functions give the same answer. Theoretical charts for the centrally loaded configurations for samples requiring hyperbolic functions as shown in Figs. 15, 16, and 17 for the respective frequencies of 8, 10 and 12 Kmc/s.

Evaluation of loss tangent (tan δ)

The loss tangent is obtained from the measurements of Q of the cavity system corresponding to two insertions of the sample differing by half a wavelength or any multiple of it inside the partially filled portion of the cavity. In fact, the process of evaluating the loss tangent from these measurements is broken up into two distinct steps, i.e., first the value of attenuation inside the partially filled portion is obtained which is later correlated to the loss tangent of the sample.

The reasons for selecting penetrations differing by half a wavelength can be understood by considering the sources of loss inside the cavity system. These sources of loss are outlined below:

(i) Losses occuring on the cavity's sidewalls ($=P_1$)

(ii) Losses occuring on the cavity's end walls ($=P_2$)

(iii) Losses occuring through the coupling holes ($=P_3$)

(iv) Losses in the material under test ($=P_4$)

(v) Losses due to the creation of higher order evanescent modes at the discontinuity ($=P_5$)

From the general definition of Q factor,

$$Q = \omega \times \frac{\text{Total stored energy in the cavity}}{\text{Power lost in the cavity}} \qquad (13)$$

where ω is the angular frequency.

For the present cavity system

$$Q = \omega \times \frac{W_1 + W_2}{P_1 + P_2 + P_3 + P_4 + P_5} \quad ---- \quad (14)$$

where w_1 is the power stored in the empty portion of the cavity while w_2 is the power stored in the partially filled portion of the cavity.

Now by inserting the dielectric rod an integral number of half wavelengths, the cavity's resonance condition is not disturbed and it remains resonant at the same frequency. Since in the present condition, the fields at the junction between the two dielectric portions and the end walls remain the same and as the coupling holes are generally kept sufficiently away from the end of the dielectric specimen inside the cavity, all the three power losses designated by P_2, P_3, P_5 remain unchanged. The change in Q results chiefly from the changes in P_1 and P_4 which will be called P_1' and P_4' for this new configuration and from the changes in the stored energy $(w_1 + w_2)$ which is now denominated as $(w_1' + w_2')$. Hence Q for this case, say Q', is given by

$$Q' = \omega \times \frac{W_1' + W_2'}{P_1' + P_4' + P_2 + P_3 + P_5} \qquad (15)$$

Hence,

$$(P_1' + P_4') - (P_1 + P_4) = \omega \left\{ \frac{W_1' + W_2'}{Q'} - \frac{W_1 + W_2}{Q} \right\} \cdots \qquad (16)$$

All these P and w terms have been expressed in terms of the various parameters of the cavity including the attenuation in the empty and partially filled portions and the following equations have been obtained correlating the attenuation with the measured Q factors. It will be shown in the appendix that:

$$\frac{\omega_r}{2} \left[\frac{X + Z_2 n \lambda_{2/2} \, d\beta_2/d\omega - Z_1 n \lambda_{1/2} \, d\beta_1/d\omega}{Q'} - \frac{X}{Q} \right]$$

$$= Z_2 \alpha_2 n \lambda_{2/2} - Z_1 \alpha_1 n \lambda_{1/2} \qquad (17)$$

where, $X = \left[Z_1 d_1' \sec^2 \beta_1 d_1' \, d\beta_1/d\omega + Z_2 l_1 \sec^2(\beta_2 l_1') \, d\beta_2/d\omega \right.$

$$\left. + \tan(\beta_1 d_1') \cdot dz_1/d\omega + \tan(\beta_2 l_1') \cdot \frac{dz_2}{d\omega} \right] \qquad (18)$$

where $\ell_1' = \ell_1 + \ell_o$ and $d_1' = d_1 + d_o$, following the convention of Equation (3). The terms Z, λ, α and β stand respectively for wave impedance, guide wavelength, attenuation and phase constants. The suffix (1) attached to these terms refers to these quantities belonging to the empty portion of the cavity while the suffix (2) refers to the partially filled portion of the cavity. d_1 and ℓ_1 refer to the lengths of the empty and the partially filled portions corresponding to the first measurement of Q when the sample was not inserted by an integral number of half wavelengths. The equation (18) simplifies considerably if one starts with a completely empty cavity, i.e., $\ell_1 = 0$. In that case, the resonance condition simplifies to

$$\beta_1 d_{1(o)} = n\pi \quad \text{------} \quad (19)$$

$$\text{and} \quad X = Z_1 d_{1(o)} d\beta_1/d\omega \text{ - - - - - - - - -} \quad (20)$$

where $d_{1(o)}$ is now the total length of the cavity.

It is possible to evaluate every term on the left hand side of Eq.(17) while α_1 can be obtained from a separate experiment, hence α_2 can be determined. It needs to be pointed out that the expressions (17) and (18) are applicable to both the configurations under consideration. It has been shown in the appendix that α_2 is related to tan δ by the following expressions.

The Side Filled Case

$$\omega^3 \mu_o^2 \epsilon_r \epsilon_o k_2^2 \tan\delta\, bt \{\phi_o(\phi_o t^2 k_1^2 - 1) + 1\}$$

$$+ 2R_m [2bk_1^2 k_2^2 + \beta^2 t \phi_1(\phi_1 - 1) + a\phi_2 k_1^2$$

$$\alpha_2 = \frac{k_1^2 k_2^2 t^2 \phi_o^2 \{\phi_1 t + \phi_2 a + \phi_3 b\}}{2\omega\mu_o\beta b [\phi_1 t(\phi_o - 1) + a k_1^2 (1 + k_2^2 \phi_o^2 t^2)]} \quad \ldots\ldots (21)$$

where $$\phi_o = \tan k_1 t / k_1 t \quad \ldots\ldots\ldots (22)$$

$$\phi_1 = k_1^2 - k_2^2 \quad \ldots\ldots\ldots (23)$$

$$\phi_2 = k_2^2 + \beta^2 \quad \ldots\ldots\ldots (24)$$

$$\phi_3 = k_1^2 + k_2^2 \quad \ldots\ldots\ldots (25)$$

R_m is the resistivity of the material of the wall of the cavity and is related to α_1 by the expression,

$$R_m = \frac{\alpha_1}{T} \quad \ldots\ldots\ldots (26)$$

where T is given by

$$T = \sqrt{\epsilon_o/\mu_o} \times \frac{1}{b} \frac{1 + 2b/a (\lambda_o/2a)^2}{\sqrt{1 - (\lambda_o/2a)^2}} \quad \ldots\ldots (27)$$

where λ_o is the free space wavelength and b is the narrow dimension of the guide.

All the other terms in the equation (21) have the same meaning as used earlier in regard to the side filled case.

The computations needed to evaluate tan δ from the measurements of Q with the use of Eqs. (17) and (21), even though simpler as compared to the corresponding equations in the earlier paper are nonetheless fairly lengthy. However, the evaluation of tan δ from Q measurements is very considerably

simplified by making the following approximations:

(i) The total energy stored in the cavity remains unaltered corresponding to the two insertions of the dielectric specimen;

(ii) The quantity $(\alpha_{2wall} - \alpha_1 \frac{Z_1^2}{Z_2^2})$ is negligible compared to $\alpha_{2(dielectric)}$ (where $\alpha_{2(dielectric)} \rightarrow \alpha_{2wall} = \alpha_2$)

By using the above approximations it will be shown that if one starts from zero insertion when $x = Z_1 d_1 d\beta_1/d\omega$ and goes to an insertion of half a wavelength inside the cavity, $\tan\delta$ may be evaluated from:

$$\frac{1}{Q'} - \frac{1}{Q} = \frac{k_2^2 \lambda_1^2 \beta_1 t_r t \tan\delta \{\phi_0(K_1^2 t^2 \phi_0 - 1) + 1\}}{2\beta_2 \lambda_1 d_{1(0)} \{\phi_1 t(\phi_0 - 1) + \alpha K_1^2 (1 + K_2^2 \phi_0^2 t^2)\}} \quad (28)$$

where $d_{1(0)}$ is the total length of the cavity at resonance corresponding to zero insertion of the cavity.

Both the approximations mentioned above are justifiable. Approximation (1) is valid due to the fact that the total length of the cavity is very much longer than half a wavelength in the partially filled portion (it may be made equal to six wavelengths or more long without any mechanical problems due to the inherent simplicity of the arrangement) and hence the difference in the stored energy in the half wavelength long section, introduced due to the dielectric insertion is pretty negligible compared to the total stored energy of the cavity. It may easily be shown from the arguments used in the derivation of the expression for α_2 that the ratio of this energy difference to the total stored energy of the empty cavity is given by:

$$\frac{\Delta W}{W} = \frac{1}{2} \frac{\left(\frac{Z_2}{Z_1} \lambda_2 \frac{d\beta_2}{d\omega} - \lambda_1 \frac{d\beta_1}{d\omega}\right)}{d_{1(0)} \frac{d\beta_1}{d\omega}} \quad \ldots\ldots \quad (29)$$

Equating the above expression to zero as stipulated in the approximation (1), for a typical set of values of λ_1, λ_2, Z_1, Z_2, $d\beta_2/dw$ and $d\beta_1/dw$ in a cavity which is five wavelengths long, results in an error of less than 1% in the evaluation of α_2. This error can be reduced in linear manner by further increasing the length of the cavity -- a requirement which can be met simply.

The second approximation introduces an error due to the neglecting of the quantity $(\alpha_{2(\text{wall})} - \alpha_1 \frac{Z_1^2}{Z_2^2})$ in comparison to $\alpha_{2(\text{dielectric})}$. As a first approximation one may assume the wall losses arising due to the imperfect conductivity remain unchanged even after the insertion of the dielectric, i.e., $\alpha_{2\text{wall}} = \alpha_1$. In addition for the usual samples, the change in the value of the wave impedance of the filled section of the cavity after insertion of dielectric sample is of the order of 2 to 4%, i.e., $Z_2 \simeq Z_1$. Hence, the quantity $\alpha_{2\text{wall}} - (\frac{Z_1}{Z_2})^2 \alpha_1$ in general turns out to be smaller than α_1 by an order of magnitude or even more. Besides, for a well silvered surface, if the insertion of the sample into the cavity, by a length equal to a half wavelength, results in the lowering of Q of the cavity by 1/3rd of its value, $\alpha_{2\text{dielectric}}$ turns out to be an order of magnitude larger than α_1. Hence, for such a case, the error introduced by the second approximation is less than 2%. Hence, in general if one uses a cavity made from a long length of well silvered waveguide, the use of the approximate equation (28) results in an error of less than five percent in the evaluation of $\tan \delta$.

This sacrifice in accuracy, which is acceptable for most of the dielectric measurements, results however, in an enormous reduction of computational work and the elimination of the need to evaluate α_1 by a separate experiment.

The Centrally Filled Case

Using the same symbols as used earlier in connection with this particular configuration

$$\alpha_2' = \frac{\omega^3 K_1'^2 K_2'^2 \epsilon_r \epsilon_0 \mu_0^2 bt \tan\delta \left\{1 + K_1'^2 d^2 \phi_0'^2 - 2/t'\, d\phi_0'\right\} + 4R_m \left\{K_1'^2 (1 + K_2'^2 d^2 \phi_0'^2)(\phi_2' d + K_2'^2 b) + K_2'^2 \phi_3' t'/2 (1 + d^2 \phi_0'^2 K_1'^2) + \phi_0' d (2K_1'^2 K_2'^2 - \beta'^2 \phi_1')\right\}}{4\beta b \mu_0 \omega \left\{K_1'^2 d + K_2'^2/2 xt - \phi_0' d\, \phi_1' + K_1'^2 K_2'^2 \phi_0'^2 d (d + t/2)\right\}} \quad \text{(30)}$$

where

$$\phi_0' = \frac{\tan K_2' d}{K_2' d} \quad \text{(31)}$$

$$\phi_1' = K_1'^2 + K_2'^2 \quad \text{(32)}$$

$$\phi_2' = K_2'^2 + \beta'^2 \quad \text{(33)}$$

$$\phi_3' = K_1'^2 + \beta'^2 \quad \text{(34)}$$

once again, using the approximation mentioned earlier, one can obtain tan δ by the following expression:

$$\frac{1}{Q'} - \frac{1}{Q} = \frac{K_2'^2 K_1'^2 t' \lambda_2'^2 \beta_1' \epsilon_r \tan\delta \left(1 + K_1'^2 d^2 \phi_0'^2 - 2/t\, d\phi_0'\right)}{4 d_{1(0)} \lambda_1' \beta_2' \left[K_1'^2 d + K_2'^2/2 \cdot t' - \phi_0 d\phi_1' + K_1'^2 K_2'^2 d(d+t'/2)\right]} \quad \ldots(35)$$

Experimental Results

Measurements of permittivity have been made on various samples of teflon, plexi-glass and a vew ceramics, with values of ϵ_r ranging up to 15. Some of these measurements have been made at the frequency of 10 Kmc for which tables have been computed and the values of the parameters read directly off there. These values have been found to be in good agreement with the values available from other sources.

Typical curves of $(d + \ell)$ vs. ℓ obtained for teflon, both for the side loaded and the centrally loaded configurations have been shown in Figs. (18) and (19) respectively. The values of ϵ_r obtained from both of these were in excellent agreement.

The $(d + \ell)$ vs ℓ curve obtained for a thick sample of plexi-glass (t=.195"), in a centrally loaded configuration, for which the guide wavelength turns out to be smaller than the free space wavelength is shown in Fig. (20).

The Q_L vs ℓ curve for a side loaded configuration (teflon, t = .03") is shown in Fig. (21). The corresponding curve for the centrally loaded configuration was also similar.

The value of tan δ was obtained by taking a number of different pairs of points from Q_L vs ℓ curve and the agreement in tan δ value has been of the order of the estimated accuracy of Q measurements.

In general, the accuracy of measurement for permittivity is within 1% and the accuracy of measurement of tan δ is within ± 2%. However, if the approximate expression for the evaluation of tan δ be used, the estimated accuracy of measurement of tan δ is within ± 7%.

Discussion of Results and Conclusions

(1) From the results obtained it follows that this method is capable of giving accurate and reliable results for the required parameters and the accuracy obtained by this is comparable or better than the accuracy obtained by the other methods.

(2) It may once again be stated that all the major advantages reported in the earlier paper are retained here as enumerated below.

(i) The method of permittivity measurement has to rely on the use of a large number of datum points and as such this is a precision method in the sense defined by Oliner[15] and Altschuler. Also, tan δ may be determined from many pairs of results.

(ii) From the very nature of the arrangements used, there is a wide choice in the values of the thicknesses of the samples that could be investigated. This technique because of the possibility of using two different configurations and the possibility of using hyperbolic functions for centrally loaded configuration gives a wide range in the values of the permittivities that could be measured.

(iii) All the measurements are made at a fixed frequency which considerably simplifies the experimental work.

(iv) Once again, the errors introduced due to the uneven finish of the end of the sample in the cavity and the tilted end walls of the cavity are obviated.[16]

(3) The relative simplicity in the computational efforts is a distinct advantage of this method over the previous one. For most of the requirements where the accuracy of $\pm 7\%$ is adequate for tan δ measurement, the

use of the approximate expression drastically reduces the computations for the evaluation of tan δ. In the majority of the cases, tan δ will be given within 5% by the use of the approximate expression.

(4) The method does not suffer from the problems encountered with the excitation of unwanted modes into the cavity.

(5) It may be mentioned that this method may very profitably be used for investigating the magnetic dielectric-like ferrites by suitably combining the measurements on a thin ferrite sample, first by placing it along the sidewalls and then by placing it along the center. This technique with the facility to position the sample in the maxima of electric or magnetic field may be a very useful method for the investigation of thin films.

Acknowledgements

Thanks are due to Dr. N. B. Bhatt, Director, Solid State Physics Lab., Delhi, for permission to start this work, and also to Mr. G. P. Sharma for his help in the initial stages of this work. Thanks are particularly due to Professor H. C. Bourne, Jr. Chairman, Electrical Engineering Department, Rice University for making available the facilities of the laboratory and workshop of his department where most of the reported work has been done.

References

(1) Lamb, J., "Dielectric Measurement at Wavelength Around 1cm by Means of an HO_1 Cylindrical Cavity Resonator", Proceedings IEE, Vol. 93, 1946, Pt. III A, p. 1447.

(2) Horner, F., Taylor, T. A. Dunsmuir, R., Lamb, J., and Jackson, W., "Resonance Methods of Dielectric Measurements at Centimetric Wavelengths", Ibid 1946, 93, Pt. III, p. 53.

(3) Collie, C. H., Hasted, J. B. and Ritson, D. M., "The Cavity Resonator Method of Measuring the Dielectric Constants of Polar Liquids in the Centimeter Band", Proceedings Physical Society, Vol. 60, 1948, p. 71.

(4) Sinha, J. K., and Brown, J., "A New Cavity Resonator Method of Measuring Permittivity", Proc. IEE, Vol. 107, Part B, Nov. 1960, p. 522.

(5) Hotston, E.S., "Correction Terms for Dielectric Measurements with Cavity Resonators", J. of Scientific Instruments, Vol. 38, 1961, p. 13

(6) Feenberg, E., "Relation Between Nodal Positions and Standing Wave Ratio in a Complex Transmission Systems, J. of Applied Physics, Vol. 17, No. 6, 1946, p. 530.

(7) Marcuvitz, N., "Waveguide Handbook", Radiation Laboratory Series, Vol. 10, McGraw Hill, 1951, Chapter 3.

(8) Collin, R. E. & Brown, J., "The Calculation of the Equivalent Circuit of an Axially Unsymmetrical Waveguide Junction", Proceedings IEE, Monograph No. 145R, August 1955 (103C, p. 121).

(9) Sinha, J.K., "A Method for the Evaluation of Equivalent Circuit Parameters of an Asymmetric Waveguide Junction", Ibid, Monograph No. 381E, May 1960.

(10) Pincherle, L. "Electromagnetic Waves in Metal Tubes Filled Longitudinally with Two Dielectrics, Physical Review, 1944, 66, p. 118.

(11) Collins, R. E., "Field Theory of Guided Waves", McGraw-Hill Book Co. 1960, p. 228

(12) Vartanian, P. H., Apres, E.P. & Gelgesson, A. L., "Propagation in Dielectric Slab Loaded Rectangular Wave Guide", IRE Trans. on Microwave Theory & Techniques, April 1958, p. 215.

(13) Montgomery, C. G., Dicke, R. H. & Purcell, E.M.,"Principles of Microwave Circuits", Chpt. 2, Radiation Laboratory Series, Vol. 8, 1948.

(14) Sinha, J.K., "A New Cavity Resonator Method of Measuring Dielectric Constants", London University, Ph.D. Thesis, 1959.

(15) Oliner, A.A. = Altschuler, H.M., "Methods of Measuring Dielectric Constants Based on Microwave Network viewpoint", Journal Applied Physics, Vol. 26, 1955, p. 214

Appendices

1. Evaluation of the Total Stored Energy $(W_1 + W_2)$ and the Losses $(P_1 + P_2)$

The steps required in deriving the Eq. (17) from Eq. (16) for expressing the attenuation α_2 in terms of Q and Q' are given below.

For the evaluation of stored energy $(W_1 + W_2)$, the cavity system is represented by the equivalent circuit shown in Fig. (22). The lengths d_1' and ℓ_1' as shown are different from the corresponding physical lengths by the amounts d_o and ℓ_o, respectively, due to the phase effects introduced at the junction. As the cavity system is being considered at resonance, the equivalent transmission system is short circuited at both the ends.

For calculating the stored energy, the two sections shown in the circuit of Fig. 2, having different propagation constants are considered separately. Consider now the section to the right of the junction plane A shown in Fig.(23) and

choose the coordinates in such a manner that the distances away from the short circuit are considered negative while the short circuit is at the plane $Z = 0$. S_2 represents the cross sectional area of the system at the plane A and n is the direction normal to S_2.

For the system under consideration if E_2 and H_2 represent the transverse components of the electric and magnetic field at the plane A, it can be shown that:

$$E_2(\text{trans}) = D_2 \sin(\beta_2 Z)\, \underline{e}_2(x,y) \qquad (36)$$

and

$$H_2(\text{trans}) = jY_2 D_2 \cos(\beta_2 Z)\, \underline{e}_2(x,y) \qquad (37)$$

In the above equations D_2 and Y_2 are respectively the amplitude coefficient and the wave impedance while $\underline{e}_2(x,y)$ is the function giving the variation of the fields in the x,y plane.

It can be shown[13] by proper operations on the Maxwell equation that:

$$\int (E \times \delta H - \delta E \times H) \cdot \underline{n}\, ds = -j\, 4\, \delta\omega_r \times \text{Total Stored energy} \qquad (38)$$

Applying this result to the system under consideration, it is seen that the only contribution to the surface integral S as shown in the Eq. (38), arises due to the cross section area S_2 at the plane A. After carrying through the mathematical operations, it is found that the energy W_2 stored in the section to the right of plane A as shown in Fig. (16) is given by

$$W_2 = \frac{1}{4} D_2^2 \left\{ l_1' Y_2 \, d\beta_2/d\omega - \frac{dY_2}{d\omega} \frac{\sin 2\beta_2 l_1'}{2} \right\} \int_{S_2} \underline{e}_2^2 \, ds_2 \qquad (39)$$

Similarly, the energy stored in the section shown to the left of plane A in Fig. (15) is given by

$$W_1 = \frac{1}{4} D_1^2 \left\{ d_1' Y_1 \, d\beta_1/d\omega - \frac{dY_1}{d\omega} \frac{\sin 2\beta_1 d_1'}{2} \right\} \int_{S_1} e_1^2 \, ds_1 \quad \text{---(40)}$$

Before writing the expression for the total energy $(W_1 + W_2)$, it is convenient first to find the relation between the amplitude constants D_1 and D_2 in the two sections by applying the Poynting Theorem which is expressed for a lossless cavity as:

$$\int_S (\underline{E} \times \underline{H}) \cdot n \cdot ds = \frac{1}{2} j\omega \int_V (\mu |\underline{H}|^2 - \epsilon |\underline{E}|^2) \, dv \quad \text{---(41)}$$

where S is the surface area and V the volume of the cavity, but S being a clased conductor in the case of a cavity. Eq. (41) is equal to zero, hence the total stored magnetic energy is equal to the total stored electric energy.

Applying these results to the system under consideration, it is found that

$$\int_{S_1} (\underline{E}_1 \times \underline{H}_1) \cdot n \, ds_1 = - \int_{S_2} (\underline{E}_2 \times \underline{H}_2) \cdot n \, ds_2 \quad \text{---(42)}$$

Putting in the values of E_2, H_2 from equations (36) and (37), the eq. (42) gives

$$\frac{D_2^2}{D_1^2} \frac{\int_{S_2} \underline{e}_2^2 \, ds_2}{\int_{S_1} \underline{e}_1^2 \, ds_1} = - \frac{\sin(2\beta_1 d_1')}{\sin(2\beta_2 l_1')} \cdot \frac{Y_1}{Y_2} \quad \text{---(43)}$$

Using these results together with the result of Eq. (3), the total energy $W = W_1 + W_2$ is given by:

$$W_1+W_2 = \frac{1}{8} D_1^2 Y_1^2 \frac{\sin(2\beta_1 d_1)}{\tan(\beta_1 d_1)} \left[Z_1 \sec^2(\beta_1 d_1) d_1' \frac{d\beta_1}{d\omega} + Z_2 l_1' \sec^2(\beta_2 l_1') \frac{d\beta_2}{d\omega} + \tan(\beta_1 d_1') \frac{dZ_1}{d\omega} + \tan(\beta_2 l_1') \frac{dZ_2}{d\omega} \right] \int_{S_1} e_1^2 \, ds_1 \quad \cdots (44)$$

Consider now the case when the dielectric rod is pushed further inside by an amount equal to $\frac{\lambda_2}{2}$ and then this reduces by $\frac{\lambda_1}{2}$, in order to maintain resonance, for such a situation, as the fields remain undistorted, the amplitude constants D_1 & D_2 remain unchanged. If the new lengths be called l_1' and d_1', it can easily be seen that:

$$\sec^2(\beta_1 d_1') = \sec^2(\beta_1 d_1) \;\&\; \sec^2(\beta_2 l_1') = \sec^2(\beta_2 l_1)$$

Hence, carrying through the same arguments as before, it can be seen that the total energy $W_1' + W_2'$ in this configuration is given by

$$W_1'+W_2' = \frac{1}{8} D_1^2 Y_1^2 \frac{\sin(2\beta_1 d_1')}{\tan(\beta_1 d_1')} \int_{S_1'} e_1^2 \, ds_1 \cdot \left[X + \frac{Z_2}{2} \lambda_2 \sec^2(\beta_2 l_1') \frac{d\beta_2}{d\omega} - \frac{Z_1}{2} \lambda_1 \sec^2(\beta_1 d_1') \frac{d\beta_1}{d\omega} \right] \quad (45)$$

where

$$X = Z_1 d_1' \sec^2(\beta_1 d_1') \frac{d\beta_1}{d\omega} + Z_2 l_1' \sec^2(\beta_2 l_1') \frac{d\beta_2}{d\omega} + \tan(\beta_1 d_1') \frac{dZ_1}{d\omega} + \tan(\beta_2 l_1') \frac{dZ_2}{d\omega} \quad \cdots (46)$$

Substituting the value of $W_1 + W_2$ and $W_1' + W_2'$ from equations (44), (45) in Eq. (16) gives

$$\frac{1}{8} D_1^2 \gamma_1^2 \frac{\sin(2\beta_1 d_1')}{\tan(\beta_1 d_1')} \int_{S_1} e_1^2 dS_1 \times \left[\frac{X + \frac{Z_2 \lambda_2}{2} \sec^2(\beta_2 l_1') \frac{d\beta_2}{d\omega} - Z_1 \frac{\lambda_1}{2} \sec^2(\beta_1 d_1')}{\varphi_2} - \frac{X}{\varphi_1} \right]$$

$$= \frac{1}{\omega} (\text{Transmission losses in length } \frac{\lambda_2}{2} - \text{transmission loss in } \frac{\lambda_1}{2}) \quad (47)$$

Consider now the losses in $\frac{\lambda_2}{2}$ section. This $\frac{\lambda_2}{2}$ section may be assumed to be equivalent to a cavity with zero end wall impedances, as only the transmission losses are to be evaluated. As the Q of this section is quite high, it will be a perfectly valid assumption to take the impedance of this cavity to be zero at resonance. This gives

$$\tanh(\gamma_2 \lambda_2/2) = 0 \quad (48)$$

where γ_2, the propagation constant in that section $= \alpha_2 + j\beta_2$ (49)

The Q of this section may be evaluated by making the resonant frequence ω_r complex and equate it to $\omega_r' + jp$, ω_r' and p being its real and imaginary components respectively. It has been shown[13] that Q of the cavity is equal to

$$Q = \frac{\omega_r}{2p} \quad (50)$$

Since ω_r is assumed to be complex, hence β_2 also becomes complex and equal to:

$$\beta_2 = \beta_2' + jp \frac{d\beta_2}{d\omega} \quad (51)$$

Hence

$$\gamma_2 = j\beta_2' + (\alpha_2 - p \cdot \frac{d\beta_2}{d\omega}) \quad (52)$$

Substituting this value of γ_2 into Eq. (48) and using Taylor's expansion, one obtains

$$\rho = \frac{\alpha_2}{d\beta_2/d\omega} \tag{53}$$

and therefore :

$$\varphi = \omega_r \frac{d\beta_2/d\omega}{2\alpha_2} \tag{54}$$

Using the definition of Q as given in Eq. (13), it follows that the energy lost in the section $\frac{\lambda_2}{2} = 2\alpha_2 x$

$$\text{Energy stored in length } \lambda_2/2 \,/\, d\beta_2/d\omega - - - \tag{55}$$

Using the expression for stored energy as given in Eq. (39), the

$$\text{transmission losses in } \frac{\lambda_2}{2} \text{ section} = \frac{1}{4} D_2^2 \alpha_2 \lambda_2 \gamma_2 \int_{S_2} e_2^2 ds_2 \tag{56}$$

Similarly the transmission losses in

$$\frac{\lambda_1}{2} \text{ section} = \frac{1}{4} D_1^2 \alpha_1 \lambda_1 \gamma_1 \int_{S_1} e_1^2 ds_1 - - - - - \tag{57}$$

Hence, transmission Losses in length $\frac{\lambda_2}{2}$ - Transmission Losses in $\frac{\lambda_1}{2}$ =

$$\frac{1}{4} D_1^2 \gamma_1^2 \int_{S_1} e_1^2 ds_1 \frac{\sin 2\beta_1 d_1'}{\tan \beta_1 d_1'} \left[Z_2 \alpha_2 \lambda_2 \sec^2(\beta_2 l_1') - Z_1 \alpha_1 \lambda_1 \sec^2(\beta_1 d_1') \right] \tag{58}$$

Using the result of Eq. (58) in Eq. (47), one obtains,

$$\frac{\omega_r}{2} \left[\frac{X + Z_2 \frac{\lambda_2}{2} \sec^2(\beta_2 l_1') \frac{d\beta_2}{d\omega} - Z_1 \frac{\lambda_1}{2} \sec^2(\beta_1 d_1') \cdot \frac{d\beta_1}{d\omega}}{\varphi_2} - \frac{X}{\varphi_1} \right]$$

$$= Z_2 \alpha_2 \frac{\lambda_2}{2} \sec^2(\beta_2 l_1') - Z_1 \alpha_1 \frac{\lambda_1}{2} \sec^2(\beta_1 d_1') \tag{59}$$

It may be mentioned that the above analysis is also applicable if l_1 is changed by any multiple of λ_2 or by $n\lambda_2$. This results in the general form of the above equation as given in Eq. (18).

As the equations (18) and (20) contain both the angles $\beta_1 d_1'$ and $\beta_2 \ell_1'$, for the simplicity in computations it is found desirable to eliminate one of the angles by using the Equation (3).

From the generality of the foregoing derivations it is easy to see that the above equations are valid both for the sidefilled and the end filled cases.

2. Evaluation of the terms $d\beta_1/d\omega$ and $d\beta_2/d\omega$.

The term $\frac{d\beta_1}{d\omega}$ appearing in the above equation is evaluated very simply by differentiating the simple waveguide equation written below

$$\beta_1^2 = \omega^2 \mu_o \epsilon_o - K_c^2 \tag{60}$$

where K_c is a constant being equal to $\frac{2\pi}{\lambda_c}$.

Hence

$$\frac{d\beta_1}{d\omega} = \omega \mu_o \epsilon_o / \beta_1 \tag{61}$$

$\frac{d\beta_2}{d\omega}$ on the other hand is a more complicated function of a, t, K_1 and K_2. Consider first the side filled case. Differentiating the equations (7') and (8'), one obtains:

$$\beta_2 \frac{d\beta_2}{d\omega} = \omega \mu_o \epsilon_o - K_2 \frac{dK_2}{d\omega} = \omega \mu_o \epsilon_1 - K_1 \frac{dK_1}{d\omega} \tag{62}$$

Similarly, differentiating Eq. (6),

$$\frac{d\phi_1}{dK_1} = - \frac{d\phi_2}{dK_2} \cdot \frac{dK_2}{d\omega} \tag{63}$$

from the equations (62) and (63), it is easy to see that

$$\omega \mu_o \epsilon_1 - \omega \mu_o \epsilon_o = \left[\frac{K_1 \frac{d\phi_2}{dK_2} + K_2 \frac{d\phi_1}{dK_1}}{d\phi_2/dK_2} \right] \cdot \frac{dK_1}{d\omega} \tag{64}$$

Putting the value of $\left(\frac{dK_1}{d\omega}\right)$ from Eq. (64) into Eq. (62), one gets

$$\frac{d\beta_2}{d\omega} = \frac{\omega\mu_0\epsilon_0}{\beta_2}\left[\frac{K_1\frac{d\phi_2}{dK_2} + K_2\epsilon_r\frac{d\phi_1}{dK_1}}{K_1\frac{d\phi_2}{dK_2} + K_2\, d\phi_1/dK_1}\right] \quad \ldots (65)$$

where

$$\frac{d\phi_1}{dK_1} = \frac{t(K_1t)\sec^2(K_1t) - t\cdot\tan(K_1t)}{K_1^2t^2} \quad \ldots (66)$$

and

$$d\phi_2/dK_2 = \frac{(a-t)K_2t\sec^2K_2(a-t) - t\tan K_2(a-t)}{K_2^2t^2} \quad (67)$$

In a similar manner, $\frac{d\beta_2'}{d\omega}$ for the centrally filled case is obtained from the Equations (9), (10) and (11) and one obtains

$$\frac{d\beta_2'}{d\omega} = \frac{\omega\mu_0\epsilon_0}{\beta_2'}\left[\frac{K_1'\cdot 2d/t'\frac{d\phi_2'}{dK_2'} - K_2'\epsilon_r\frac{d\phi_1'}{dK_1'}}{K_1'2d/t'\frac{d\phi_2'}{dK_2'} - K_2'\, d\phi_1'/dK_1'}\right] \quad \ldots (68)$$

where

$$\frac{d\phi_1'}{dK_1'} = -\left[\frac{K_1't'\,\mathrm{Cosec}^2 K_1't'/2 + 2\cot K_1't'/2}{K_1'^2t'}\right] \quad (69)$$

and

$$\frac{d\phi_2'}{dK_2'} = \left[\frac{K_2'd\sec^2(K_2'd) - \tan K_2'd}{K_2'^2d}\right] \quad \ldots (70)$$

3. Correlation of α_2 with $\tan\delta$.

The attentuation constant (α) in a transmission system is defined as

$$\alpha = \frac{\text{Rate of power dissipation}}{2 \times \text{Power flowing in the cross section}} \quad \ldots (71)$$

$$= \frac{\frac{dP}{dz}}{2P} \quad \ldots (72)$$

For the case under consideration $\frac{dP}{dz}$ consists of two parts, $\frac{dP}{dz}_{(conductor)}$, i.e., the power loss due to the finite conducting of the metallic walls and $\frac{dP}{dz}_{(diel)}$, i.e., the power losses due to the dielectric sample itself.
It is known that:

$$\frac{dP}{dz}_{(Conductor)} = \frac{R_m}{2} \int_S |H_t|^2 \, ds \quad - - - \quad (73)$$

where R_m is the surface resistivity and $|Ht|$ is the magnetic field which is tangential to the walls. The integration is carried out for the entire surface area/unit length of the transmitting guide.

$$\frac{dP}{dz}_{(dielectric)} = \frac{1}{2} \omega \epsilon_r \epsilon_o \tan\delta \int_V |E|^2 dv \cdot - - \quad (74)$$

tan δ in the above equation is the loss tangent term to be evaluated from the value of α_2 and the integration is done at the volume occupied by the dielectric specimen per unit length.

Finally,

$$P = \frac{1}{2} \int_{x=0}^{x=b} \int_{y=0}^{y=a} E_x H_y^* \, dx \cdot dy. \quad (75)$$

where E_x and Hy^* are the tangential components of the fields and the integration is carried out over the cross section of the waveguide.

Putting the values of the fields :

the Equations (73), (74) and (75) one obtains the correlation of α_2 with tan δ for the sidefilled case as given in Equation (21).

Similarly, putting the values of the fields :

in the Equations (73), (74) and (75), one obtains the corresponding expression for α_2 in terms of tan δ for the centrally filled case as given in equation (28).

4. Derivation of the approximate relation for the evaluation of tan δ.

If the first measurement of Q, say Q_1, corresponds to zero insertions and the second measurement, say Q_2, to half wavelength insertion, it follows then from Eq. (17), ignoring the difference in stored energy in the two situations:

$$\frac{\omega_r}{2}\left(\frac{X}{Q_2} - \frac{X}{Q_1}\right) = Z_2\alpha_2\frac{\lambda_2}{2} - Z_1\alpha_1\frac{\lambda_1}{2} \qquad (76)$$

Now putting the value of $X = \frac{Z_1 d_{1(o)}\omega\mu_o\epsilon_o}{\beta_1}$ from equations (20) and (61), when $d_{1(o)}$ is the resonant length of the empty cavity

$$d_{1(o)}\frac{\omega^2\mu_o\epsilon_o}{\beta_1}\left(\frac{1}{Q_2} - \frac{1}{Q_1}\right) = \frac{Z_2}{Z_1}\alpha_2\lambda_2 - \alpha_1\lambda_1 \qquad (77)$$

Hence

$$\frac{Z_1}{Z_2}\frac{\omega^2\mu_o\epsilon_o}{\lambda_2}d_{1(o)}\left(\frac{1}{Q_2} - \frac{1}{Q_1}\right) = \alpha_2 - \alpha_1\frac{Z_1}{Z_2}\frac{\lambda_1}{\lambda_2} \qquad (78)$$

Now if α_2 is written as $\alpha_{2(wall)} + \alpha_{2(diel)}$, one easily obtains the Eq. (28) from the Eqs. (21) and (78), where Q' and Q correspond to Q_2 and Q_1, respectively, if $\{\alpha_{2(wall)} - \alpha_1\ \lambda_1^2/\lambda_2^2\}$ be ignored in comparison α_2(dielectric).

5. As mentioned earlier, Q of the cavity is obtained at a fixed frequency by the tuning plunger by keeping ℓ fixed and varied. The relation between δd and δf, the corresponding frequency charge, is obtained by differentiating Eq. (3) which gives

$$\frac{\delta f}{\delta d} = \frac{\beta_1\left[\frac{Z_2^2}{Z_1^2}\sec^2(\beta_2\ell') + \left(\frac{Z_1^2 - Z_2^2}{Z_1^2}\right)\right]}{\sec^2(\beta_2\ell')\left\{\frac{Z_2}{Z_1}\cdot\ell'\frac{d\beta_2}{df} + \frac{Z_2^2}{Z_1^2}d'\,d\beta_1/df\right\} + \tan(\beta_2\ell')\frac{d}{df}(Z_2/Z_1) + \left(\frac{Z_1^2 - Z_2^2}{Z_1^2}\right)\cdot\frac{d\beta_1}{df}} \qquad (79)$$

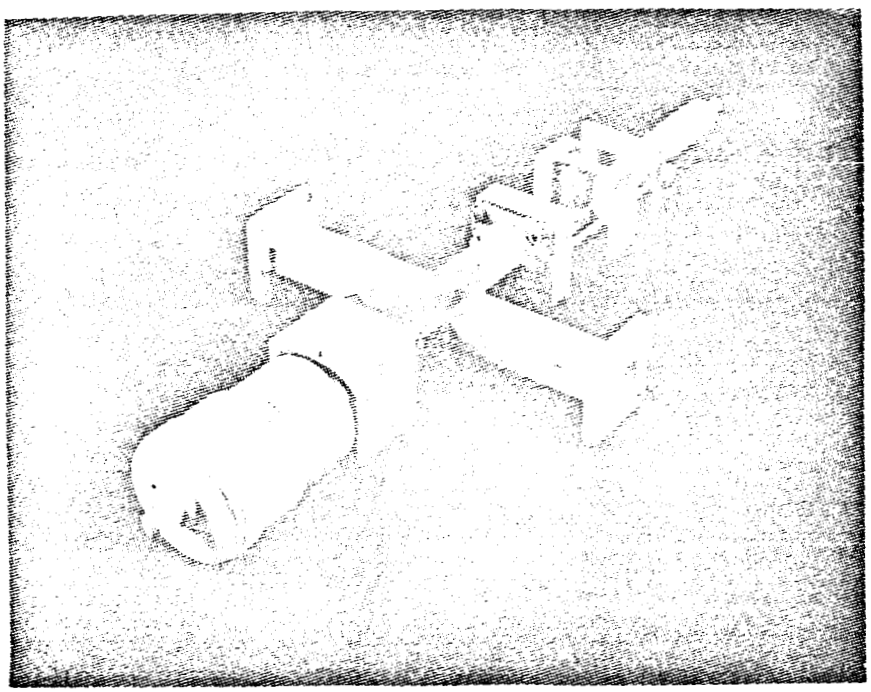

Fig. I - Photograph of the Cavity System

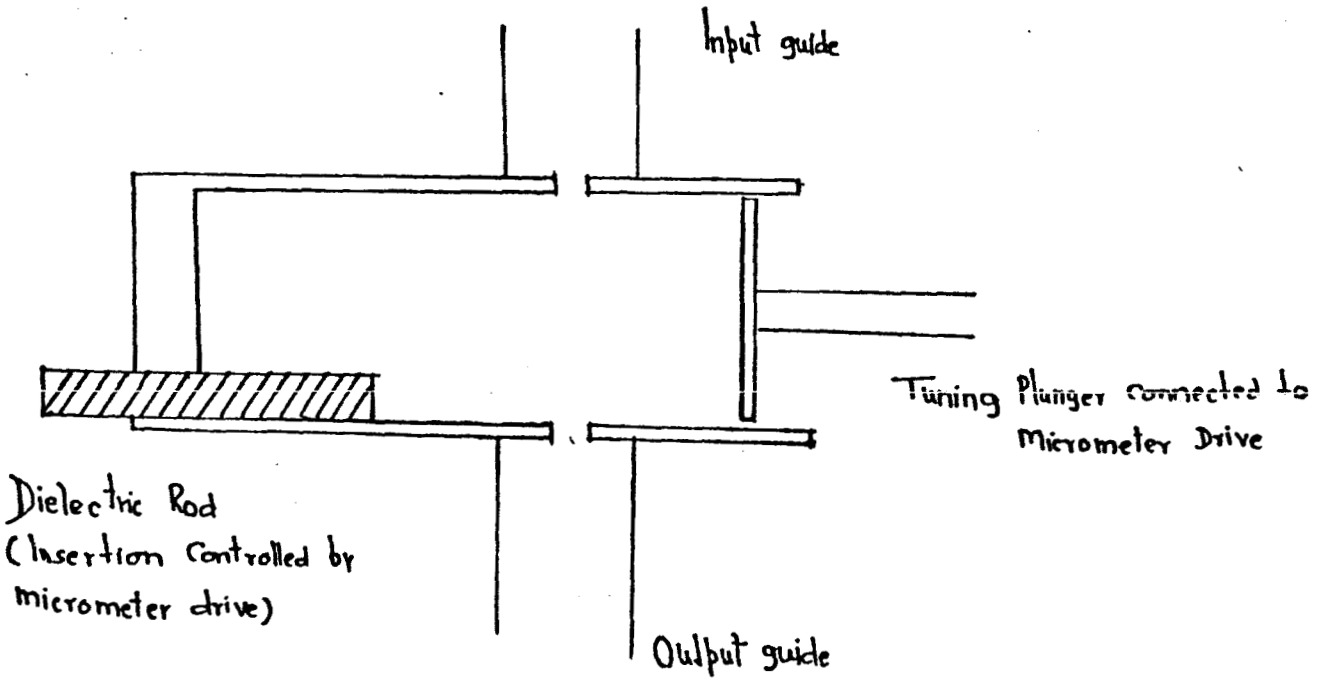

Fig 2. — General arrangement of the cavity & the sample

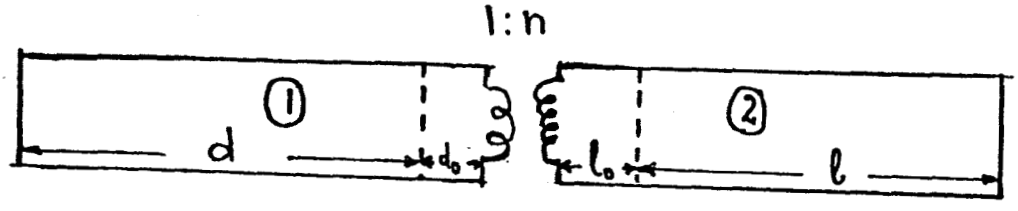

Fig 3 — Equivalent circuit for the cavity

(Transmission lines (1) & (2) represent the H_{01} modes in the empty & partially filled portions of the cavity respectively)

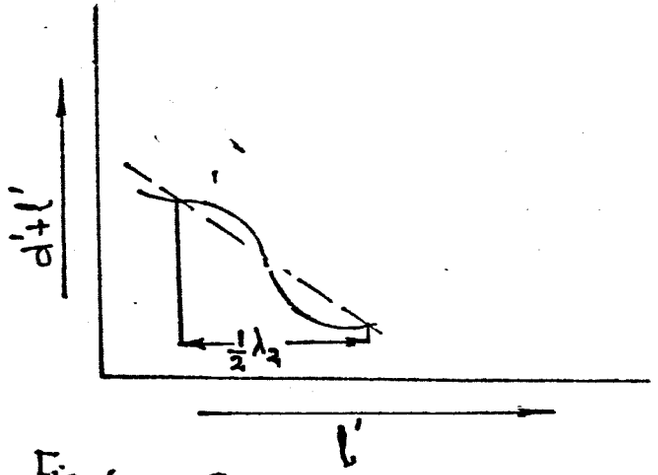

Fig 4— General shape of the curve showing the dependence of (d'+l') on l'.

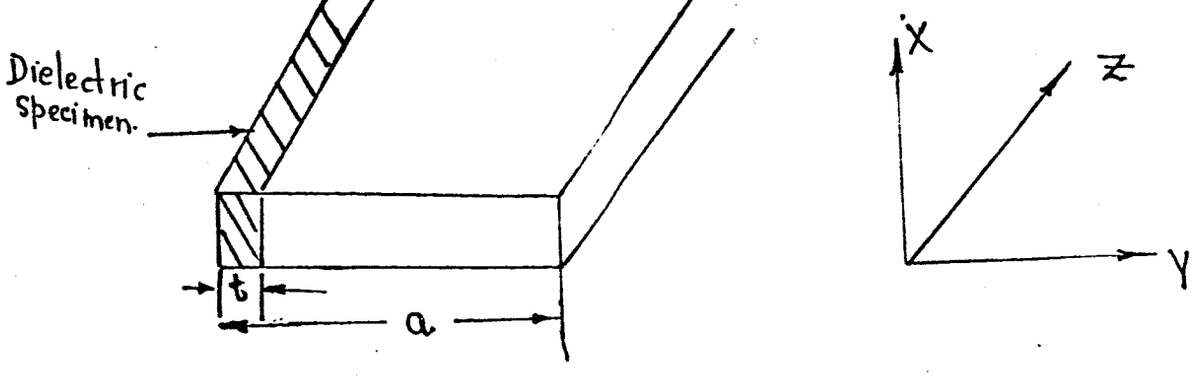

Fig 5— Arrangement showing the sample along the cavity's side wall.

Wavelength Permittivity Table (Frequency: 8kmc)

Thickness (inches)	.025	.05	.075	.1	.125	.150	.175	.20	.225	.250	.275	.30	.325	.35
Wavelength (λg) cems	Permittivity													
4.20	219.45	55.49												
4.30	217.97	54.78	24.75	14.30	9.50									
4.40	216.41	54.04	24.28	13.96	9.24	6.69	5.17							
4.50	214.78	53.27	23.79	13.62	8.97	6.48	5.00	4.05	3.41					
4.60	213.05	52.46	23.29	13.26	8.70	6.27	4.83	3.90	3.28	2.84				
4.70	211.20	51.61	22.76	12.90	8.43	6.05	4.65	3.76	3.16	2.74	2.43			
4.80	209.22	50.71	22.22	12.52	8.15	5.84	4.48	3.62	3.04	2.64	2.34	2.13		
4.90	207.08	49.76	21.65	12.13	7.87	5.62	4.30	3.47	2.92	2.54	2.26	2.05		
5.00	204.77	48.74	21.04	11.73	7.57	5.40	4.13	3.33	2.80	2.44	2.17	1.98	1.83	
5.10	202.24	47.65	20.41	11.31	7.27	5.17	3.95	3.19	2.69	2.34	2.09	1.90	1.77	1.66
5.20	199.45	46.48	19.74	10.87	6.96	4.94	3.77	3.05	2.57	2.24	2.01	1.83	1.70	1.60
5.30	196.36	45.21	19.03	10.41	6.64	4.71	3.60	2.91	2.46	2.15	1.93	1.77	1.64	1.55
5.40	192.91	43.82	18.26	9.93	6.31	4.47	3.41	2.77	2.34	2.05	1.85	1.70	1.59	1.50
5.50	189.03	42.31	17.45	9.42	5.97	4.22	3.23	2.62	2.23	1.96	1.77	1.63	1.53	1.45
5.60	184.60	40.63	16.57	8.89	5.62	3.97	3.05	2.48	2.12	1.87	1.70	1.57	1.48	1.41
5.70	179.50	38.78	15.63	8.33	5.25	3.72	2.86	2.34	2.00	1.78	1.62	1.51	1.42	1.36
5.80	173.56	36.70	14.60	7.73	4.87	3.45	2.67	2.20	1.89	1.69	1.55	1.45	1.37	1.32
5.90	166.53	34.37	13.49	7.10	4.47	3.18	2.47	2.05	1.78	1.60	1.48	1.39	1.32	1.27
6.00	158.03	31.71	12.26	6.42	4.05	2.91	2.28	1.91	1.67	1.52	1.41	1.33	1.27	1.23
6.10	147.72	28.66	10.92	5.70	3.62	2.62	2.08	1.76	1.56	1.43	1.34	1.27	1.23	1.19
6.20	134.69	25.12	9.43	4.93	3.16	2.33	1.88	1.62	1.45	1.35	1.27	1.22	1.18	1.15
6.30	117.79	20.96	7.78	4.10	2.69	2.02	1.67	1.47	1.34	1.26	1.20	1.16	1.14	1.11
6.40	95.00	16.00	5.93	3.21	2.19	1.71	1.47	1.32	1.24	1.18	1.14	1.11	1.09	1.08

Fig 6

Wavelength Permittivity Table (frequency 10 kmc)

Thickness (inches) → / Wavelength (cms) ↓	.025	.05	.075	.1	.125	.150	.175	.200	.225	.250	.275	.30	.325	.35
							Permittivity							
3.25	139.74	35.44	16.23	9.54										
3.30	138.60	34.89	15.88	9.29	6.27	4.64	3.67							
3.35	137.34	34.30	15.51	9.02	6.07	4.48	3.54	2.93	2.52					
3.40	135.94	33.65	15.10	8.74	5.85	4.31	3.40	2.82	2.43	2.15				
3.45	134.35	32.93	14.66	8.43	5.62	4.13	3.26	2.70	2.33	2.07	1.88			
3.50	132.54	32.12	14.17	8.10	5.38	3.95	3.11	2.58	2.22	1.98	1.80	1.67		
3.55	130.42	31.19	13.63	7.73	5.12	3.75	2.95	2.45	2.12	1.89	1.73	1.60	1.51	
3.60	127.90	30.12	13.01	7.33	4.83	3.53	2.78	2.32	2.01	1.80	1.65	1.54	1.45	1.39
3.65	124.83	28.86	12.31	6.88	4.52	3.30	2.61	2.18	1.90	1.71	1.57	1.47	1.40	1.34
3.70	120.97	27.34	11.49	6.37	4.17	3.05	2.42	2.03	1.78	1.61	1.49	1.40	1.34	1.29
3.75	115.94	25.47	10.52	5.78	3.78	2.78	2.22	1.88	1.66	1.51	1.41	1.34	1.28	1.24
3.80	109.07	23.09	9.34	5.10	3.35	2.48	2.00	1.72	1.54	1.41	1.33	1.27	1.22	1.19
3.85	99.04	19.93	7.89	4.30	2.85	2.15	1.77	1.55	1.40	1.31	1.24	1.20	1.16	1.14
3.90	82.92	15.52	6.03	3.33	2.28	1.78	1.52	1.36	1.26	1.20	1.16	1.13	1.10	1.09

Fig 7

Wavelength Permittivity Table (frequency 12 kmc)

Thickness (inches) → / Wave length (λg) (cms) ↓	.025	.05	.075	.1	.125	.15	.175	.20	.225	.250	.275	.30	.325	.350
							Permittivity							
2.62	97.76	25.14												
2.66	96.62	24.60	11.38	6.79	4.69	3.55								
2.70	95.28	23.96	10.98	6.51	4.47	3.38	2.73	2.32	2.04					
2.74	93.64	23.21	10.51	6.18	4.23	3.19	2.58	2.19	1.93	1.75	1.61			
2.78	91.56	22.28	9.96	5.80	3.95	2.98	2.41	2.05	1.81	1.65	1.53	1.44	1.38	
2.82	88.75	21.09	9.27	5.35	3.63	2.73	2.22	1.90	1.69	1.55	1.44	1.37	1.31	1.27
2.86	84.70	19.46	8.37	4.78	3.24	2.45	2.01	1.73	1.56	1.44	1.35	1.29	1.24	1.21
2.90	78.15	17.06	7.15	4.05	2.76	2.12	1.76	1.55	1.41	1.32	1.25	1.21	1.17	1.14
2.94	65.44	13.10	5.33	3.05	2.14	1.70	1.47	1.33	1.24	1.19	1.15	1.12	1.10	1.08
2.98	28.98	5.10	2.30	1.57	1.30	1.18	1.12	1.08	1.06	1.04	1.03	1.03	1.02	1.02

Fig 8

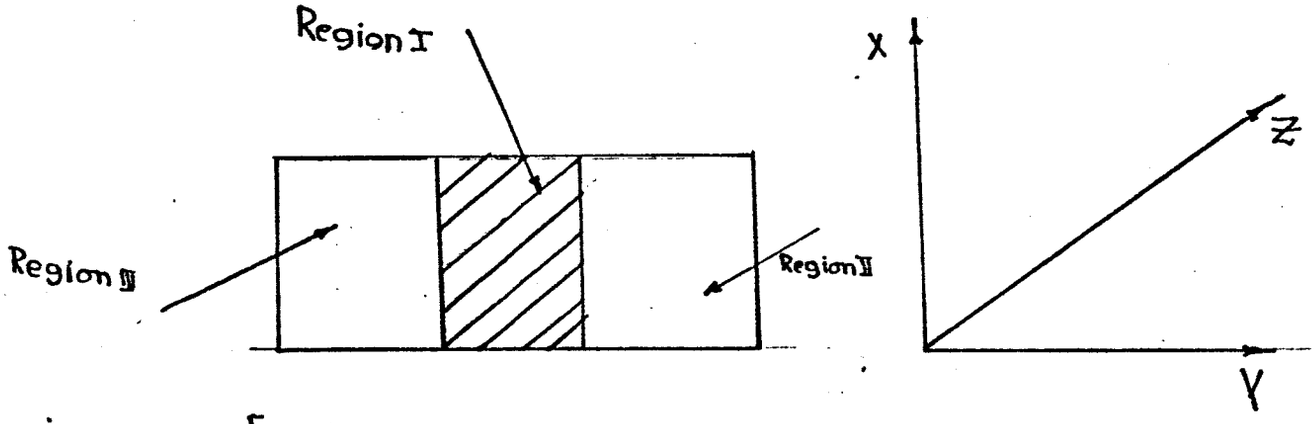

Fig(9) – Cross section of the cavity system when the dielectric is placed along the center of the cross section

Wavelength Permittivity Table (frequency 8 kmc)

Thickness (cms) → / Wavelength (cms) ↓	.03	.05	.08	.10	.13	.15	.18	.20	.23	.25	.28	.30	.33	.36	.38
							Permittivity								
3.80	25.26	13.22	9.21	7.20	6.00	5.20	4.62	4.20	3.86	3.60	3.38	3.20	3.04	2.91	2.80
3.90	56.47	17.34	10.58	7.81	6.29	5.34	4.69	4.21	3.85	3.57	3.34	3.15	2.99	2.86	2.74
4.00	54.78	16.29	9.96	7.36	5.95	5.06	4.45	4.00	3.66	3.39	3.18	3.00	2.85	2.73	2.62
4.10	51.29	15.29	9.37	6.94	5.62	4.79	4.21	3.80	3.48	3.23	3.03	2.86	2.73	2.61	2.51
4.20	47.96	14.34	8.81	6.54	5.31	4.53	3.99	3.61	3.31	3.08	2.89	2.73	2.61	2.50	2.40
4.30	44.81	13.44	8.28	6.16	5.01	4.29	3.79	3.42	3.15	2.93	2.76	2.61	2.49	2.39	2.30
4.40	41.81	12.58	7.78	5.81	4.73	4.06	3.59	3.25	3.00	2.79	2.63	2.50	2.38	2.29	2.21
4.50	38.95	11.77	7.30	5.46	4.47	3.84	3.41	3.09	2.85	2.66	2.51	2.39	2.28	2.19	2.12
4.60	36.23	10.99	6.84	5.14	4.21	3.63	3.23	2.94	2.72	2.54	2.40	2.28	2.19	2.10	2.03
4.70	33.64	10.26	6.41	4.83	3.97	3.43	3.06	2.79	2.59	2.42	2.29	2.19	2.10	2.02	1.95
4.80	31.17	9.55	6.00	4.54	3.75	3.25	2.90	2.65	2.46	2.31	2.19	2.09	2.01	1.94	1.88
4.90	28.81	8.88	5.61	4.26	3.53	3.07	2.75	2.52	2.35	2.21	2.10	2.01	1.93	1.86	1.81
5.00	26.56	8.24	5.23	3.99	3.32	2.90	2.61	2.40	2.23	2.11	2.01	1.92	1.85	1.79	1.74
5.10	24.42	7.63	4.87	3.74	3.12	2.74	2.47	2.28	2.13	2.01	1.92	1.84	1.78	1.72	1.68
5.20	22.36	7.05	4.53	3.50	2.94	2.58	2.34	2.16	2.03	1.92	1.84	1.77	1.71	1.66	1.61
5.30	20.40	6.49	4.21	3.27	2.76	2.44	2.21	2.05	1.93	1.84	1.76	1.69	1.64	1.60	1.56
5.40	18.52	5.96	3.89	3.05	2.59	2.30	2.10	1.95	1.84	1.75	1.68	1.63	1.58	1.54	1.50
5.50	16.72	5.45	3.60	2.84	2.42	2.16	1.98	1.85	1.75	1.67	1.61	1.56	1.52	1.48	1.45
5.60	15.00	4.96	3.31	2.63	2.27	2.03	1.87	1.75	1.67	1.60	1.54	1.50	1.46	1.43	1.40
5.70	13.35	4.50	3.04	2.44	2.12	1.91	1.77	1.67	1.59	1.53	1.48	1.44	1.40	1.38	1.35
5.80	11.77	4.05	2.78	2.26	1.97	1.79	1.67	1.58	1.51	1.46	1.42	1.38	1.35	1.33	1.31
5.90	10.26	3.62	2.53	2.06	1.83	1.68	1.58	1.50	1.44	1.39	1.36	1.33	1.30	1.28	1.26
6.00	8.80	3.21	2.29	1.91	1.70	1.57	1.48	1.42	1.37	1.33	1.30	1.28	1.25	1.24	1.22
6.10	7.41	2.81	2.06	1.75	1.58	1.47	1.40	1.34	1.30	1.27	1.25	1.23	1.21	1.19	1.18
6.20	6.06	2.43	1.83	1.59	1.46	1.37	1.31	1.27	1.24	1.22	1.19	1.18	1.16	1.15	1.14
6.30	4.78	2.07	1.62	1.44	1.34	1.28	1.23	1.20	1.18	1.16	1.15	1.13	1.12	1.11	1.11
6.40	3.54	1.72	1.42	1.30	1.23	1.19	1.16	1.14	1.12	1.11	1.10	1.09	1.08	1.08	1.07

Fig 10

Wavelength Permittivity Table (frequency 10 kmc)

Thickness (cms) → / Wavelength (cms) ↓	.03	.05	.08	.10	.13	.15	.18	.20	.23	.25	.28	.30	.33	.36	.38
								Permittivity							
.05	15.99	8.55	6.07	4.83	4.09	3.59	3.24	2.97	2.77	2.60	2.47	2.36	2.26	2.18	2.11
.10	30.46	11.08	6.91	5.20	4.26	3.68	3.27	2.98	2.76	2.58	2.44	2.32	2.22	2.14	2.07
.15	34.05	10.39	6.50	4.91	4.04	3.49	3.11	2.84	2.63	2.47	2.34	2.23	2.14	2.06	1.99
.20	31.70	9.72	6.11	4.62	3.82	3.31	2.96	2.71	2.51	2.36	2.24	2.14	2.05	1.98	1.92
.25	29.41	9.07	5.72	4.35	3.60	3.13	2.81	2.57	2.37	2.25	2.14	2.05	1.97	1.90	1.84
.30	27.17	8.43	5.35	4.08	3.39	2.96	2.66	2.45	2.28	2.15	2.05	1.96	1.89	1.83	1.77
.35	24.99	7.81	4.98	3.82	3.19	2.79	2.52	2.32	2.17	2.05	1.96	1.88	1.81	1.75	1.71
.40	22.85	7.20	4.62	3.57	2.99	2.63	2.38	2.20	2.06	1.95	1.87	1.80	1.74	1.68	1.64
.45	20.76	6.60	4.28	3.32	2.80	2.47	2.25	2.08	1.96	1.86	1.78	1.72	1.66	1.62	1.58
.50	18.72	6.02	3.94	3.08	2.61	2.32	2.12	1.97	1.86	1.77	1.70	1.64	1.59	1.55	1.51
.55	16.73	5.46	3.60	2.84	2.43	2.17	1.99	1.86	1.76	1.68	1.62	1.57	1.52	1.49	1.45
.60	14.78	4.90	3.28	2.61	2.25	2.02	1.86	1.75	1.66	1.59	1.54	1.49	1.46	1.42	1.40
.65	12.87	4.36	2.96	2.39	2.07	1.88	1.74	1.64	1.57	1.51	1.46	1.42	1.39	1.36	1.34
.70	11.01	3.83	2.65	2.17	1.90	1.74	1.63	1.54	1.48	1.43	1.39	1.36	1.33	1.31	1.29
.75	9.18	3.32	2.35	1.95	1.74	1.60	1.51	1.44	1.39	1.35	1.32	1.29	1.27	1.25	1.24
.80	7.40	2.81	2.06	1.75	1.58	1.47	1.40	1.35	1.30	1.27	1.25	1.23	1.21	1.19	1.18
.85	5.65	2.32	1.77	1.54	1.42	1.34	1.29	1.25	1.22	1.20	1.18	1.16	1.15	1.14	1.13
.90	3.94	1.83	1.48	1.34	1.26	1.22	1.18	1.16	1.14	1.13	1.11	1.10	1.10	1.09	1.08

Fig 11

Wavelength Permittivity Table (frequency 12 kmc)

Thickness (cms) → / Wavelength (cms) ↓	.03	.05	.08	.10	.13	.15	.18	.20	.23	.25	.28	.30	.33	.36	.38
								Permittivity							
2.54	11.13	6.10	4.42	3.59	3.08	2.75	2.51	2.33	2.19	2.08	1.99	1.91	1.85	1.80	1.76
2.58	24.22	7.60	4.87	3.74	3.13	2.75	2.49	2.29	2.15	2.03	1.94	1.86	1.80	1.74	1.70
2.62	21.84	6.92	4.47	3.46	2.91	2.57	2.33	2.16	2.03	1.92	1.84	1.77	1.71	1.66	1.62
2.66	19.49	6.25	4.07	3.18	2.69	2.39	2.18	2.02	1.91	1.81	1.74	1.68	1.63	1.58	1.55
2.70	17.18	5.59	3.68	2.90	2.48	2.21	2.02	1.89	1.79	1.71	1.64	1.59	1.55	1.51	1.48
2.74	14.88	4.94	3.30	2.63	2.26	2.03	1.88	1.76	1.67	1.60	1.55	1.50	1.47	1.43	1.41
2.78	12.61	4.29	2.92	2.36	2.06	1.86	1.73	1.63	1.56	1.50	1.46	1.42	1.39	1.36	1.34
2.82	10.37	3.65	2.55	2.10	1.85	1.69	1.59	1.51	1.45	1.40	1.37	1.34	1.31	1.29	1.27
2.86	8.15	3.02	2.18	1.84	1.65	1.53	1.45	1.39	1.34	1.31	1.28	1.25	1.24	1.22	1.21
2.90	5.95	2.40	1.82	1.58	1.45	1.36	1.31	1.27	1.24	1.21	1.19	1.18	1.16	1.15	1.14
2.94	3.77	1.78	1.46	1.32	1.25	1.20	1.17	1.15	1.13	1.12	1.11	1.10	1.09	1.08	1.07
2.98	1.62	1.17	1.10	1.07	1.06	1.05	1.04	1.04	1.03	1.03	1.02	1.02	1.02	1.02	1.02

Fig 12

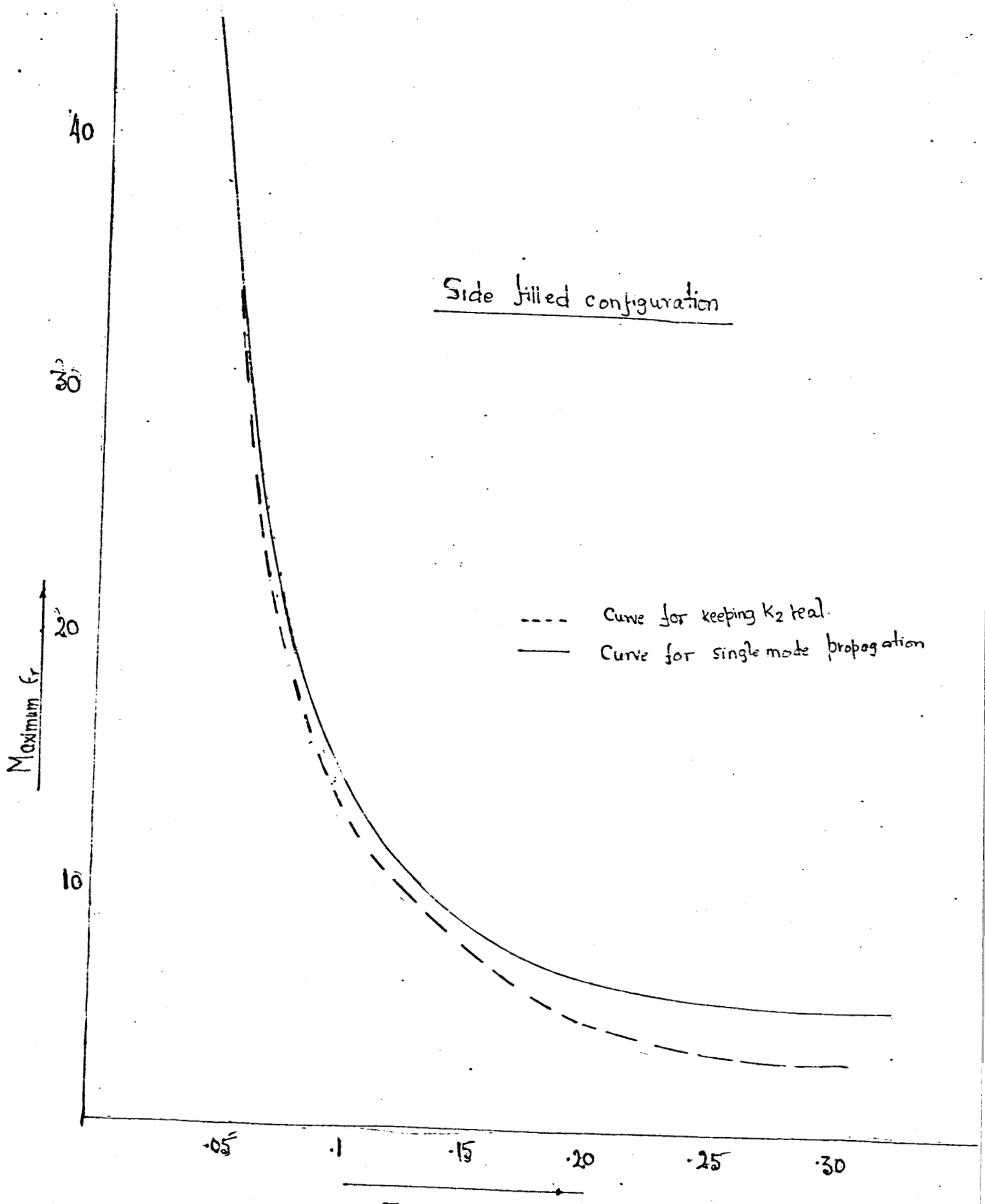

Fig 13

Theoretical curves correlation $\epsilon_{r(max)}$ with sample thicknesses for the single mode propagation and limit to the use of real functions.

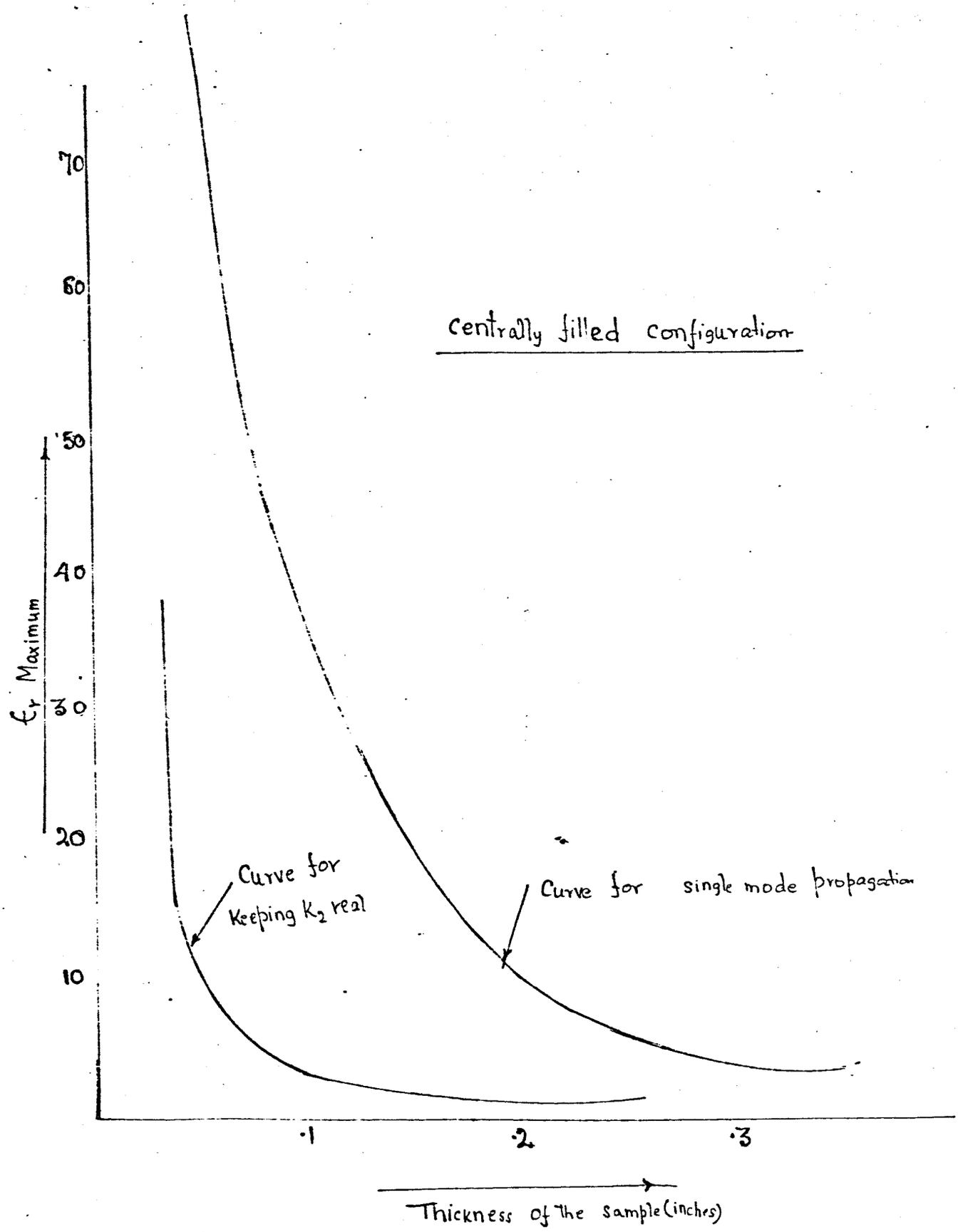

Fig 14

Theoretical curves correlating ϵ_r(max) with sample thicknesses for single mode propagation and for limit to the use of only real functions.

WAVELENGTH PERMITTIVITY TABLE (Frequency 8 kmc)

Thickness (cm) → / Wavelength (cm) ↓	.81	.76	.71	.66	.61	.56	.51	.46	.41	.36	.30	.25	.20	.15	.10
								Permittivity							
3.75	2.02	2.06	2.12	2.18	2.26	2.35	2.46	2.59	2.76	2.98	3.28	3.69	4.31	5.34	7.41
3.70	2.05	2.10	2.16	2.23	2.31	2.40	2.51	2.65	2.83	3.05	3.36	3.78	4.42	5.49	7.63
3.65	2.09	2.15	2.20	2.27	2.35	2.45	2.57	2.71	2.89	3.13	3.44	3.88	4.54	5.64	7.85
3.60	2.14	2.19	2.25	2.32	2.41	2.51	2.63	2.77	2.96	3.20	3.53	3.98	4.66	5.80	8.08
3.55	2.18	2.23	2.30	2.37	2.46	2.56	2.69	2.84	3.03	3.28	3.61	4.08	4.79	5.96	8.31
3.50	2.23	2.28	2.35	2.42	2.51	2.62	2.75	2.91	3.10	3.36	3.71	4.19	4.91	6.13	8.56
3.45	2.27	2.33	2.40	2.48	2.57	2.68	2.81	2.98	3.18	3.45	3.80	4.30	5.05	6.30	8.81
3.40	2.32	2.38	2.45	2.53	2.63	2.74	2.88	3.05	3.26	3.53	3.90	4.41	5.19	6.48	9.06
3.35	2.37	2.43	2.51	2.59	2.69	2.81	2.95	3.12	3.34	3.62	4.00	4.53	5.33	6.66	9.33
3.30	2.43	2.49	2.56	2.65	2.75	2.87	3.02	3.20	3.42	3.72	4.11	4.65	5.48	6.85	9.60
3.25	2.48	2.55	2.62	2.71	2.82	2.94	3.09	3.28	3.51	3.81	4.21	4.78	5.63	7.05	9.89
3.20	2.54	2.61	2.69	2.78	2.89	3.02	3.17	3.36	3.60	3.91	4.33	4.91	5.79	7.25	10.18
3.15	2.60	2.67	2.75	2.85	2.96	3.09	3.25	3.45	3.70	4.02	4.45	5.05	5.95	7.46	10.48
3.10	2.66	2.74	2.82	2.92	3.03	3.17	3.34	3.54	3.79	4.12	4.57	5.19	6.12	7.68	10.79
3.05	2.73	2.80	2.89	2.99	3.11	3.25	3.42	3.63	3.90	4.24	4.69	5.33	6.29	7.90	11.12
3.00	2.80	2.88	2.97	3.07	3.19	3.34	3.51	3.73	4.00	4.35	4.82	5.48	6.48	8.13	11.45
2.95	2.87	2.95	3.04	3.15	3.28	3.43	3.61	3.83	4.11	4.48	4.96	5.64	6.66	8.37	11.80
2.90	2.95	3.03	3.12	3.23	3.37	3.52	3.71	3.94	4.23	4.60	5.10	5.80	6.86	8.62	12.15
2.85	3.03	3.11	3.21	3.32	3.46	3.62	3.81	4.05	4.35	4.73	5.25	5.97	7.06	8.88	12.52
2.80	3.11	3.20	3.30	3.42	3.55	3.72	3.92	4.16	4.47	4.87	5.40	6.15	7.27	9.15	12.90
2.75	3.20	3.29	3.39	3.51	3.66	3.83	4.03	4.29	4.60	5.01	5.56	6.33	7.49	9.43	13.30
2.70	3.29	3.38	3.49	3.61	3.76	3.94	4.15	4.41	4.74	5.16	5.73	6.52	7.72	9.71	13.71
2.65	3.38	3.48	3.59	3.72	3.87	4.06	4.27	4.54	4.88	5.32	5.90	6.72	7.96	10.01	14.14
2.60	3.49	3.59	3.70	3.83	3.99	4.18	4.40	4.68	5.03	5.48	6.08	6.93	8.20	10.33	14.58
2.55	3.59	3.70	3.81	3.95	4.11	4.31	4.54	4.83	5.19	5.65	6.27	7.15	8.46	10.65	15.04
2.50	3.71	3.81	3.93	4.08	4.24	4.44	4.68	4.98	5.35	5.83	6.47	7.37	8.73	10.99	15.52
2.45	3.83	3.94	4.06	4.21	4.38	4.59	4.83	5.14	5.52	6.02	6.68	7.61	9.01	11.34	16.02

Fig 15

WAVELENGTH PERMITTIVITY TABLE (10 Kmc)

Thickness (cm) → / Wavelength (cm) ↓	.81	.76	.71	.66	.61	.56	.51	.46	.41	.36	.30	.25	.20	.15	.10
								Permittivity							
3.00	1.65	1.68	1.71	1.75	1.80	1.86	1.93	2.02	2.13	2.27	2.45	2.71	3.11	3.77	5.09
2.95	1.70	1.73	1.77	1.81	1.86	1.92	2.00	2.09	2.21	2.35	2.55	2.83	3.25	3.95	5.36
2.90	1.75	1.78	1.82	1.87	1.92	1.99	2.07	2.17	2.29	2.45	2.66	2.95	3.40	4.14	5.64
2.85	1.80	1.84	1.88	1.93	1.99	2.06	2.14	2.24	2.37	2.54	2.76	3.08	3.55	4.34	5.92
2.80	1.86	1.90	1.94	1.99	2.05	2.13	2.22	2.33	2.46	2.64	2.88	3.21	3.71	4.54	6.22
2.75	1.92	1.96	2.00	2.06	2.12	2.20	2.30	2.41	2.56	2.74	2.99	3.34	3.87	4.75	6.52
2.70	1.98	2.02	2.07	2.13	2.20	2.28	2.38	2.50	2.65	2.85	3.11	3.48	4.04	4.97	6.83
2.65	2.04	2.09	2.14	2.20	2.27	2.36	2.46	2.59	2.75	2.96	3.24	3.63	4.21	5.19	7.15
2.60	2.11	2.16	2.21	2.28	2.35	2.44	2.55	2.69	2.86	3.08	3.37	3.78	4.39	5.42	7.48
2.55	2.18	2.23	2.29	2.36	2.44	2.53	2.65	2.79	2.97	3.20	3.50	3.93	4.58	5.66	7.83
2.50	2.26	2.31	2.37	2.44	2.53	2.63	2.75	2.89	3.08	3.32	3.64	4.09	4.77	5.91	8.18
2.45	2.33	2.39	2.45	2.53	2.62	2.72	2.85	3.00	3.20	3.45	3.79	4.26	4.98	6.16	8.55
2.40	2.42	2.48	2.54	2.62	2.71	2.82	2.96	3.12	3.32	3.59	3.94	4.44	5.18	6.43	8.91
2.35	2.51	2.57	2.64	2.72	2.82	2.93	3.07	3.24	3.45	3.73	4.10	4.62	5.40	6.71	9.32
2.30	2.60	2.66	2.74	2.82	2.92	3.04	3.19	3.37	3.59	3.88	4.27	4.81	5.63	6.99	9.73
2.25	2.70	2.77	2.84	2.93	3.04	3.16	3.32	3.50	3.74	4.04	4.44	5.01	5.86	7.29	10.15
2.20	2.80	2.87	2.95	3.05	3.16	3.29	3.45	3.64	3.89	4.20	4.62	5.22	6.11	7.60	10.59
2.15	2.92	2.99	3.07	3.17	3.28	3.42	3.59	3.79	4.05	4.38	4.82	5.44	6.37	7.93	11.04
2.10	3.03	3.11	3.20	3.30	3.42	3.56	3.73	3.95	4.21	4.56	5.02	5.66	6.64	8.26	11.52
2.05	3.16	3.24	3.33	3.44	3.56	3.71	3.89	4.11	4.39	4.75	5.23	5.90	6.92	8.62	12.02
2.00	3.30	3.38	3.47	3.58	3.71	3.87	4.06	4.29	4.58	4.95	5.45	6.16	7.22	8.99	12.53
1.95	3.44	3.53	3.62	3.74	3.88	4.04	4.23	4.47	4.77	5.16	5.69	6.42	7.53	9.37	13.07
1.90	3.59	3.68	3.79	3.91	4.05	4.22	4.42	4.67	4.99	5.39	5.94	6.70	7.85	9.78	13.64
1.85	3.76	3.85	3.96	4.08	4.23	4.41	4.62	4.88	5.21	5.63	6.20	7.00	8.20	10.21	14.24
1.80	3.94	4.03	4.15	4.28	4.43	4.61	4.83	5.10	5.44	5.89	6.48	7.31	8.56	10.66	14.86
1.75	4.13	4.23	4.35	4.48	4.64	4.83	5.06	5.34	5.70	6.16	6.77	7.64	8.95	11.13	15.51
1.70	4.34	4.44	4.56	4.70	4.87	5.07	5.30	5.60	5.97	6.45	7.09	7.99	9.36	11.64	16.21

Fig 16

WAVELENGTH PERMITTIVITY TABLE (12 kmc)

Thickness (cm) → / Wavelength (cm) ↓	.81	.76	.71	.66	.61	.56	.51	.46	.41	.36	.30	.25	.20	.15	.10
								Permittivity							
2.50	1.45	1.47	1.50	1.52	1.56	1.60	1.65	1.71	1.78	1.88	2.01	2.19	2.46	2.92	3.84
2.45	1.51	1.53	1.56	1.59	1.63	1.67	1.73	1.79	1.88	1.98	2.13	2.33	2.63	3.14	4.16
2.40	1.57	1.60	1.63	1.66	1.70	1.75	1.81	1.88	1.98	2.09	2.25	2.47	2.81	3.37	4.49
2.35	1.63	1.66	1.70	1.73	1.78	1.83	1.90	1.98	2.08	2.21	2.38	2.62	2.99	3.60	4.83
2.30	1.70	1.73	1.77	1.81	1.86	1.92	1.99	2.08	2.19	2.33	2.51	2.78	3.18	3.84	5.17
2.25	1.78	1.81	1.85	1.89	1.95	2.01	2.09	2.18	2.30	2.45	2.65	2.94	3.37	4.09	5.53
2.20	1.85	1.89	1.93	1.98	2.04	2.10	2.19	2.29	2.41	2.58	2.80	3.11	3.57	4.34	5.89
2.15	1.93	1.97	2.02	2.07	2.13	2.20	2.29	2.40	2.54	2.71	2.95	3.28	3.78	4.61	6.27
2.10	2.02	2.06	2.11	2.16	2.23	2.31	2.40	2.52	2.66	2.85	3.10	3.46	3.99	4.88	6.65
2.05	2.11	2.15	2.21	2.27	2.34	2.42	2.52	2.64	2.80	3.00	3.27	3.64	4.21	5.16	7.05
2.00	2.21	2.25	2.31	2.37	2.45	2.54	2.64	2.77	2.94	3.15	3.44	3.84	4.44	5.45	7.47
1.95	2.31	2.36	2.42	2.49	2.56	2.66	2.77	2.91	3.09	3.31	3.62	4.04	4.68	5.75	7.90
1.90	2.42	2.47	2.54	2.61	2.69	2.79	2.91	3.06	3.24	3.48	3.80	4.26	4.93	6.07	8.34
1.85	2.54	2.60	2.66	2.74	2.82	2.93	3.06	3.21	3.41	3.66	4.00	4.48	5.20	6.40	8.80
1.80	2.67	2.73	2.79	2.87	2.97	3.08	3.21	3.38	3.58	3.85	4.21	4.71	5.47	6.74	9.28
1.75	2.80	2.87	2.94	3.02	3.12	3.24	3.38	3.55	3.77	4.05	4.43	4.96	5.76	7.10	9.79
1.70	2.95	3.02	3.09	3.18	3.28	3.41	3.55	3.74	3.97	4.27	4.66	5.23	6.07	7.48	10.31
1.65	3.11	3.18	3.26	3.35	3.46	3.59	3.74	3.94	4.18	4.49	4.91	5.50	6.39	7.88	10.86
1.60	3.28	3.36	3.44	3.53	3.65	3.78	3.95	4.15	4.41	4.74	5.18	5.80	6.74	8.30	11.44
1.55	3.47	3.55	3.63	3.73	3.85	4.00	4.17	4.38	4.65	5.00	5.46	6.11	7.10	8.75	12.05
1.50	3.68	3.75	3.85	3.95	4.08	4.23	4.41	4.63	4.91	5.27	5.76	6.45	7.49	9.22	12.71
1.45	3.90	3.96	4.08	4.19	4.32	4.48	4.67	4.90	5.19	5.58	6.09	6.81	7.90	9.73	13.40
1.40	4.15	4.23	4.33	4.45	4.58	4.75	4.95	5.19	5.50	5.90	6.44	7.20	8.35	10.27	14.13
1.35	4.42	4.51	4.61	4.73	4.88	5.05	5.26	5.51	5.84	6.26	6.83	7.62	8.83	10.85	14.92
1.30	4.72	4.81	4.92	5.05	5.20	5.38	5.60	5.86	6.21	6.65	7.24	8.08	9.35	11.48	15.75
1.25	5.05	5.15	5.26	5.40	5.55	5.74	5.97	6.25	6.61	7.07	7.70	8.58	9.92	12.16	16.67

Fig 17

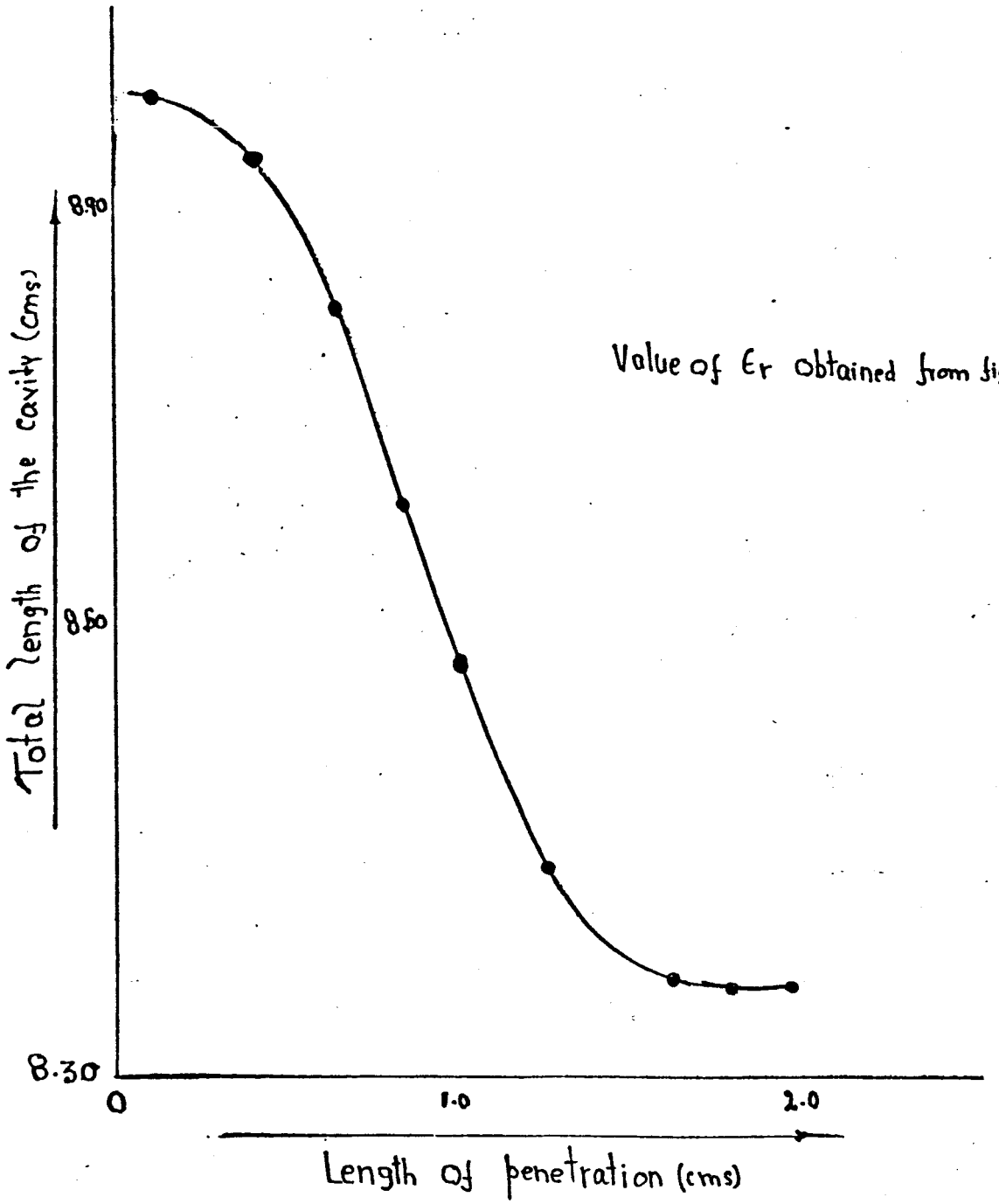

Value of ϵ_r obtained from fig(8) = 2.26

Fig(8) — Variation of the total length of the cavity with dielectric insertion for the side filled configuration ($t = .3''$)

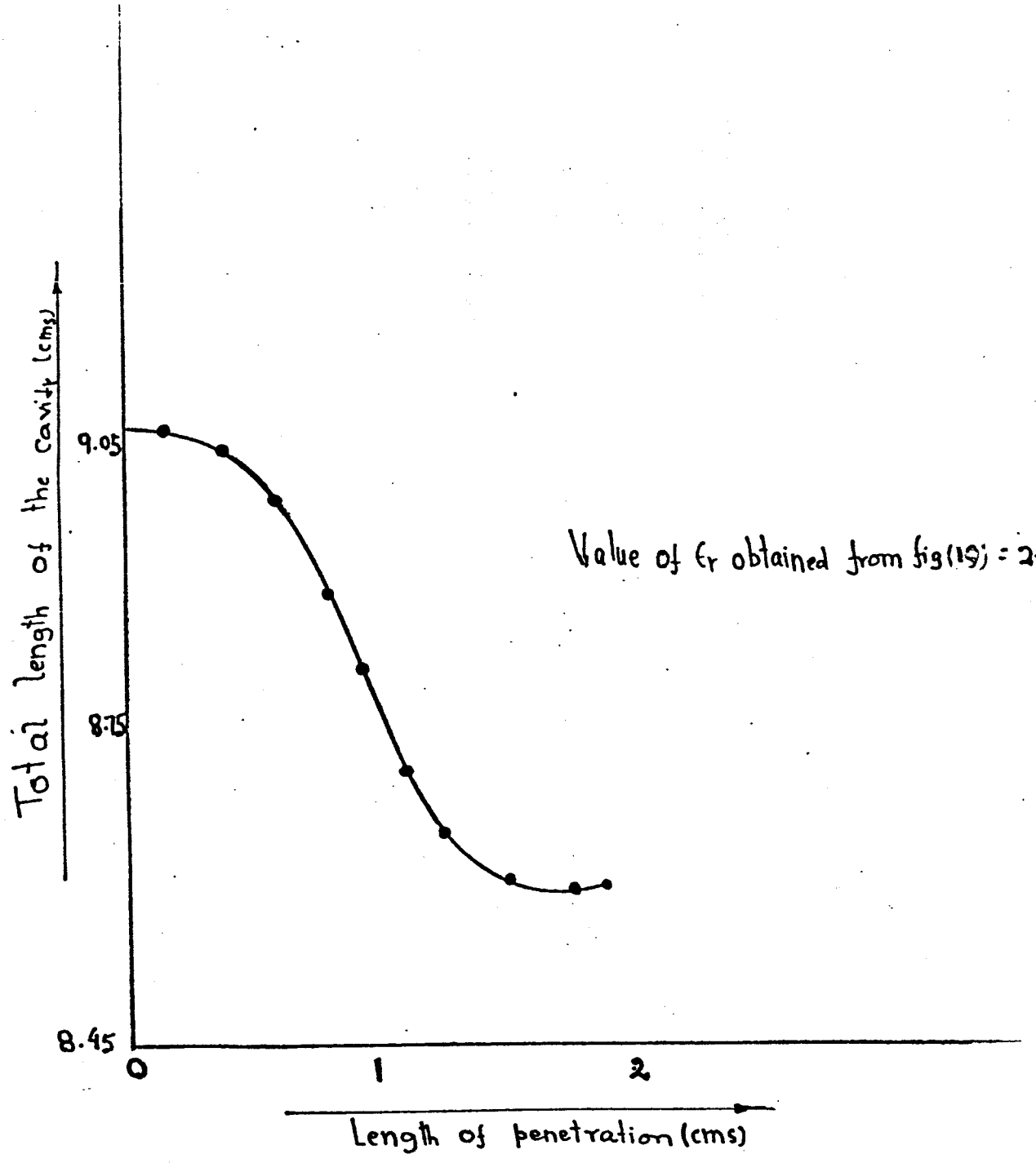

Value of ϵ_r obtained from fig(19) = 2.26

Fig 19- Variation of total length of the cavity with dielectric insertion for the centrally filled configuration t'=.1".

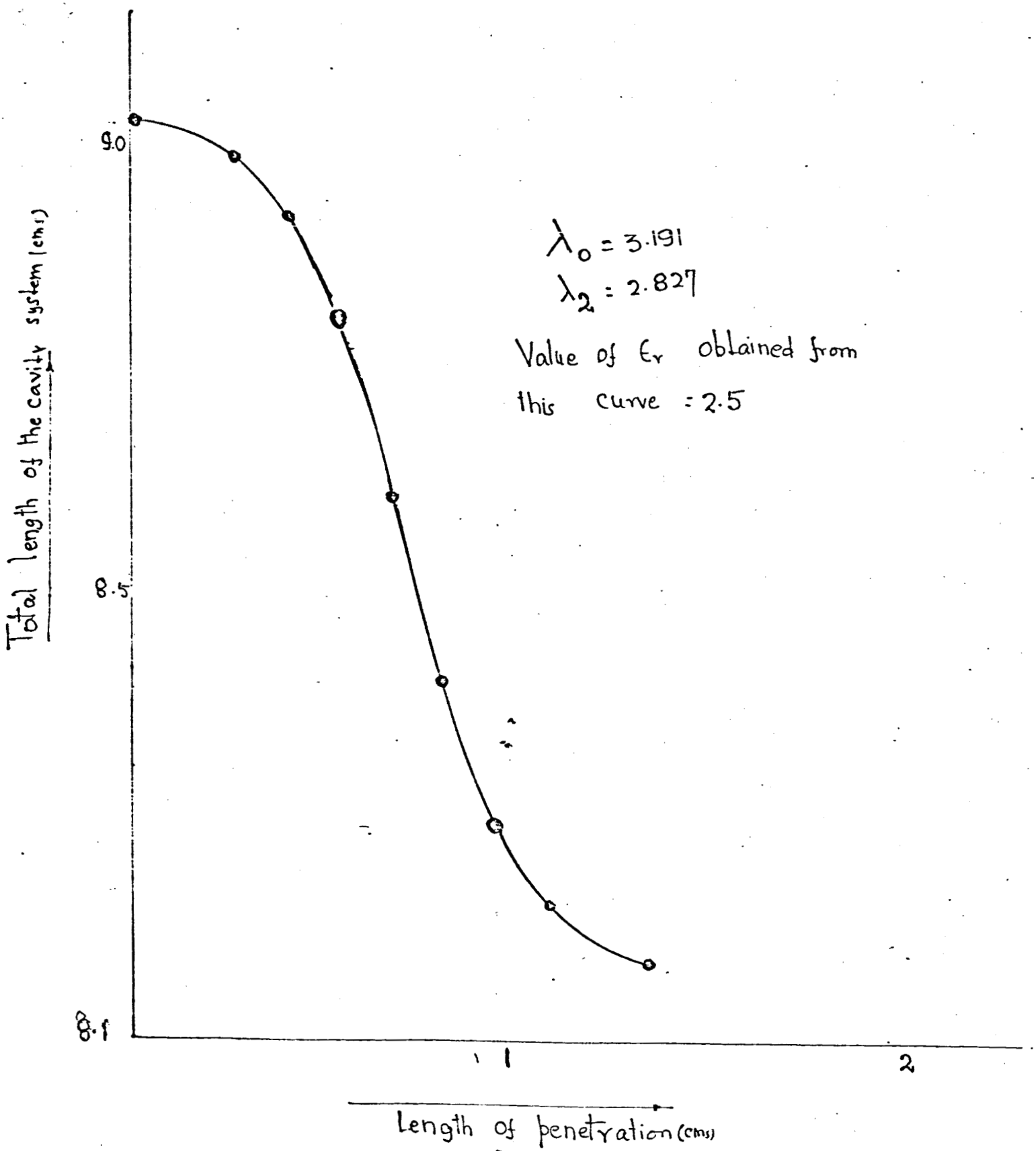

$\lambda_0 = 3.191$

$\lambda_2 = 2.827$

Value of ϵ_r obtained from this curve = 2.5

Fig (20)

Variation of total length of the cavity with dielectric insertion for centrally loaded configuration for a sample of plexiglass ($t' = .195''$).

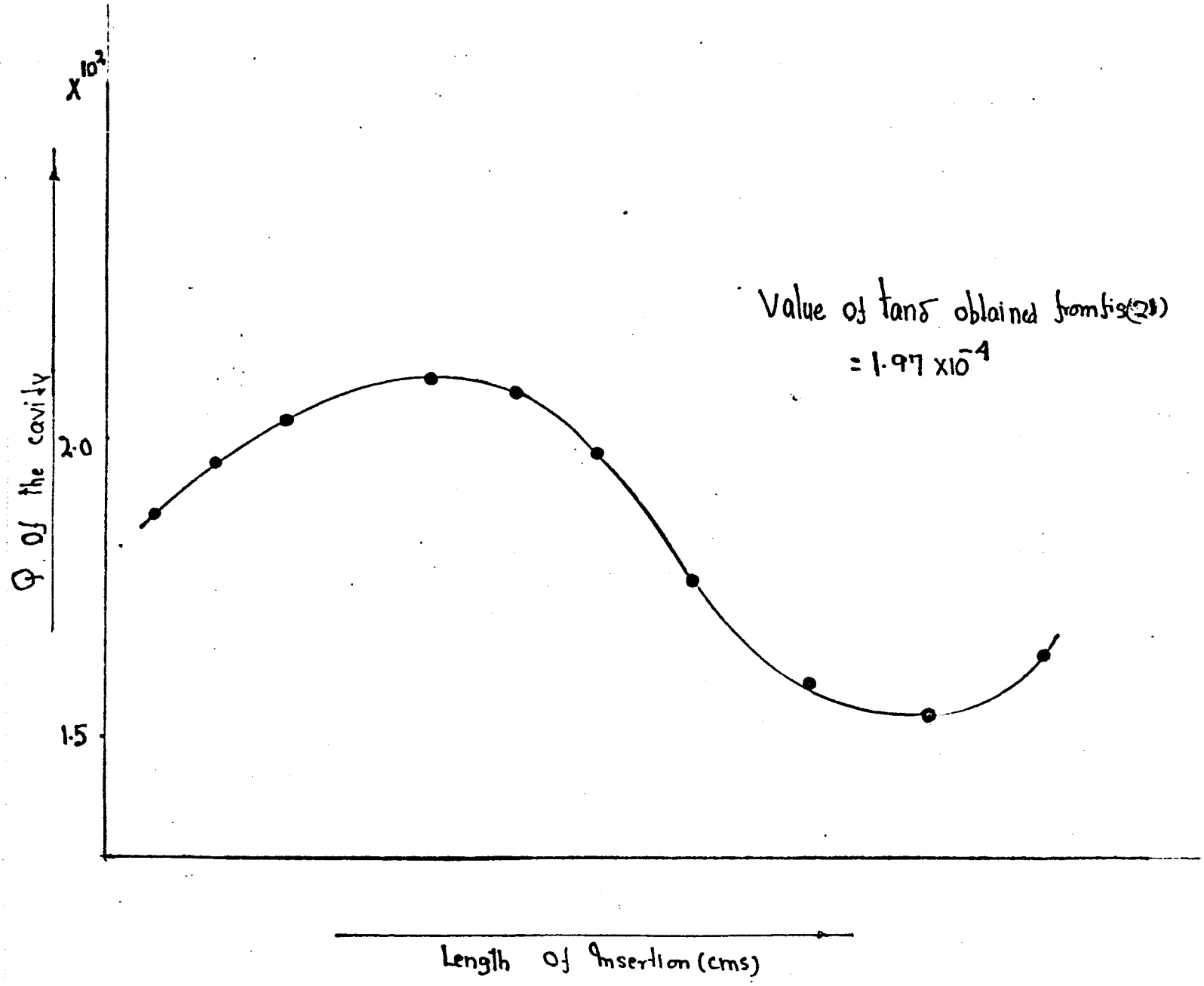

Fig(21) —— Variation of Q with the length of insertion for the side filled configuration (t = 0.3")